

# Variability in the bio-optical properties of Mayagüez Bay

by

Marcos A. Rosado Torres

A thesis submitted in partial fulfillment  
of the requirements for the degree of

MASTER OF MARINE SCIENCE

in

Biological Oceanography

UNIVERSITY OF PUERTO RICO  
MAYAGUEZ CAMPUS  
2000

Approved by:

---

Fernando Gilbes, Ph. D.  
Member, Graduate Committee

---

Date

---

Jorge R. García-Sais, Ph. D.  
Member, Graduate Committee

---

Date

---

Roy A. Armstrong, Ph. D.  
President, Graduate Committee

---

Date

---

Alexander Leyderman, Ph. D.  
Representative of Graduate Studies

---

Date

---

Dallas Alston, Ph. D.  
Chairperson, Department of Marine Sciences

---

Date

---

Jaime Seguel, Ph. D.  
Director of Graduate Studies

---

Date

## **Abstract**

Particulate absorption coefficients, colored dissolved organic matter absorption coefficients, backscattering coefficients, remote sensing reflectance, chlorophyll-a concentration and salinity were measured during several cruises in Mayagüez Bay from February 1997 to October, 1999. The principal purpose of this study was to quantify temporal and spatial variability in both apparent and inherent optical properties and to examine the sources of such variability. High temporal and spatial variability was found for all the bio-optical properties. Several optical provinces were identified. The dominance of colored dissolved organic matter and detritus absorption over phytoplankton absorption suggests that ocean color is highly influenced by river input in the bay. High chlorophyll concentration associated with highly light-attenuating waters suggests that phytoplankton communities may be limited by light during the rainy season.

## Resumen

Los coeficientes de absorción de partículas, coeficientes de absorción de materia orgánica disuelta coloreada, coeficientes de retro-dispersión, reflectancia tele-detectada, concentración de clorofila-a y salinidad fueron medidos durante varios cruceros a la Bahía de Mayagüez desde febrero 1997 hasta octubre 1999. El propósito principal de este estudio fue cuantificar la variabilidad temporal y espacial en las propiedades ópticas tanto aparentes como inherentes y examinar las fuentes de esta variabilidad. Una alta variabilidad temporal y espacial fue encontrada en todas las propiedades bio-ópticas. Varias provincias ópticas fueron identificadas. La dominación de la absorción de materia orgánica disuelta coloreada y la absorción de detrito sobre la absorción de fitoplancton sugiere que el color del océano es altamente influenciado por el insumo ribereño en la bahía. Altas concentraciones de clorofila asociadas a aguas con alta atenuación de luz sugieren que las comunidades de fitoplancton en la bahía podrían estar limitadas por la luz.

## **Acknowledgements**

I would like to thank my parents, Rafael and Gloria and my brother Robert, I simply adore you. I would like to acknowledge my friends, Fernando, Jesús, Ramón and Patrick who guided me through this process and were always there. I would also like to thank my graduate committee, Dr. Roy Armstrong, Dr. Fernando Gilbes and Dr. Jorge R. García-Sais, for their support and guidance. Capt. Dennis Corales assistance in the field operations is genuinely appreciated. Last but not least, I would like to thank all those who provided support, knowledge and hope through this journey. This research was supported by NASA grants NAG13-99029 and NAG13-54.

## TABLE OF CONTENTS

LIST OF TABLES .....	vi
LIST OF FIGURES.....	vii
BACKGROUND .....	1
INTRODUCTION .....	6
OBJECTIVES .....	9
METHODS .....	10
FIELD WORK.....	10
LABORATORY WORK.....	12
DATA ANALYSIS.....	14
RESULTS .....	16
INHERENT OPTICAL PROPERTIES.....	16
APPARENT OPTICAL PROPERTIES.....	34
ANCILLARY DATA .....	44
DISCUSSION.....	51
CONCLUSION.....	57
REFERENCES .....	58

## LIST OF TABLES

Table 1. Analysis of Variance (two-way, without replicates) between stations and months for the absorption coefficients (S. = Significant, N.S = Non significant). P equals probability of no statistically significant differences.....	21
Table 2. Absorption coefficients of CDOM ( $a_g$ ) at 412 and 443 nm and spectral slopes during July 98 and October 99. ....	24
Table 3. Analysis of Variance (two-way, without replicates) between stations and months for the backscattering coefficient (S. = Significant, N.S = Non significant). P equals probability of no statistically significant differences.....	32
Table 4. Correlation between backscattering coefficient and selected parameters.....	32
Table 5. Vertical attenuation coefficient and estimated euphotic zone in Mayagüez Bay during July 1998.....	43
Table 6. Vertical attenuation coefficients at 490 nm calculated for the Yagüez River transect during October 1999.....	45

## LIST OF FIGURES

Figure 1.	Stations sampled during 1997 and 1998 cruises in Mayagüez Bay.....	9
Figure 2.	Stations sampled on October, 1998. Stations 1 to 6 were sampled on October 19 and Stations 7 to 11 on October 24.....	13
Figure 3.	Absorption coefficients at surface for Atuneras station from February 1997 to January 1998.....	17
Figure 4.	Particulate absorption coefficient ( $a_p$ ) at surface in Añasco station from February 1997 to January 1998.....	18
Figure 5.	Detritus absorption coefficient ( $a_d$ ) at surface in Añasco station (a) and Oceánica station (b) from February 97 to January 98.....	19
Figure 6.	Spectra of $a_p$ , $a_d$ , $a_{ph}$ and $a_{ph}^*$ in Mayagüez Bay during July 98. The legend at the top right corner applies to all graphs.....	22
Figure 7.	Spectra of $a_g$ in Mayagüez Bay during July 1998.....	23
Figure 8.	Spectra of $a_p$ , $a_d$ , $a_{ph}$ and $a_{ph}^*$ for stations 1 to 6 during October 1999. The legend at the top right corner applies to all graphs.....	25
Figure 9.	Spectra of $a_p$ , $a_d$ , $a_{ph}$ and $a_{ph}^*$ for stations 8 to 11 during October 1999. The legend at the top right corner applies to all graphs.....	27
Figure 10.	Spectra of $a_g$ in Mayagüez Bay during October 99.....	28

Figure 11. Profiles of the backscattering coefficient for Atuneras and Añasco stations for November 1997 (top), December 1998 (middle) and January 1998(bottom). The legend at the top right corner applies to all graphs.....	29
Figure 12. Relationship of $b_b$ and wavelengths measured in Mayagüez Bay from November 1997 to January 1998. Legend at the top right corner applies to all graphs.....	30
Figure 13. Linear fits and correlation coefficients of $b_b$ vs. $a_p$ at the selected wavelengths.....	31
Figure 14. Profiles of the backscattering coefficient for Oceánica(a), Manchas (b), Atuneras (c), Añasco (d), Acueductos (e) and Rodríguez (f) in Mayagüez Bay during July 98. The legend at the top right corner applies to all graphs.....	33
Figure 15. Profiles of the backscattering coefficient for selected stations in the Guanajibo River cruise, October 1998. The legend at the top right corner applies to all graphs.....	35
Figure 16. Selected backscattering profiles from the Yagüez River transect during October 1998. The legend at the top right corner applies to all graphs.....	36
Figure 17. First meter average of total absorption coefficient ( $m^{-1}$ ) and beam attenuation coefficient ( $m^{-1}$ ) in Yagüez River stations, October 1999 ...	37

Figure 18. Remote sensing reflectance curves from June 1997 to January 1998.....	38
Figure 19. The three typical spectral shapes of remote sensing reflectance (Rrs) curves obtained in Mayagüez Bay. These examples are from November 1997. Notice the difference in magnitudes of the y axis.....	40
Figure 20. Remote sensing reflectance curves in Mayagüez Bay during July 1998.....	41
Figure 21. Remote sensing reflectance curves for the Guanajibo River stations (stations 1-6), and the Yagüez River stations (stations 7-11) during October 1999.....	42
Figure 22. Chl-a concentrations and salinities at surface in Mayagüez Bay during the October 1999 cruise.....	46
Figure 23. River discharge, salinity and Chl-a measured in Mayagüez Bay from February 1997 to January 1998 .....	48
Figure 24. Suspended particulate matter (SPM) at surface in Mayagüez Bay during October 1999.....	49
Figure 25. Comparison of particulate absorption coefficient, detritus absorption coefficient and phytoplankton absorption coefficient at 443 nm. Note the proportion of particulate absorption due to detritus.....	52

## **BACKGROUND**

Absorption and scattering are collectively known as inherent optical properties because they are defined for collimated light and thus independent of radiance distribution (Kirk, 1994). Values of absorption and scattering vary greatly among natural waters due to the differences in kinds and concentrations of dissolved and particulate substances. These differences underlie the wide variations in apparent properties of natural waters. These properties, namely the vertical attenuation coefficient (K), radiance (L), irradiance (E) and reflectance (R) are functions of the radiance distribution as well of the inherent properties (Weidemann and Bannister, 1986). To better understand these properties, the dissolved and particulate components of the ecosystem must be identified and their contributions to absorption and scattering evaluated.

Absorption occurs when a photon passes in the vicinity of a molecule and is captured, increasing its energy by an amount corresponding to the energy of the photon (Kirk, 1994). Most of the light energy absorbed in the aquatic medium ends up as heat or as chemical energy in the form of photosynthetically produced biomass. Only a tiny part is turned back into light again by fluorescence and even this is for the most part re-absorbed before it can escape from the system (Kirk, 1994). Absorption in the aquatic ecosystem can be attributed to four components: water, colored dissolved organic matter, phytoplankton and inanimate particulate matter (tripton). Water absorbs very weakly in the blue and green regions of the spectrum but its absorption begins to rise above 550 nm and is very high in the red region (Pope and Fry, 1997). The contribution of water itself to the attenuation of PAR by absorption of quanta is of importance only above 500 nm. Salts present in sea water have no significant effect on absorption in the visible/photosynthetic range. The result of microbial decomposition of plant

tissue is a complex group of compounds, collectively named humic substances (Kirk, 1994). Sometimes they are called Gelbstoff, meaning “yellow substance” in German, a more acceptable term being colored dissolved organic matter (CDOM). These substances enter the marine environment as the result of river input and coastal runoff, although a fraction of the total marine Gelbstoff is produced *in situ*. These compounds are yellow to brown in color and absorb light in the blue end of the spectrum, absorbing strongly ultraviolet wavelengths (Carder et. al, 1989). If present in large concentrations, they can reduce the photosynthetically active radiation available to phytoplankton, reducing primary production (D’sa et. al, 1999). Detritus or inanimate particulate matter absorbs low in the red region of the spectrum and increases exponentially into the blue region. The spectral shape is very similar to that of CDOM and in some waters it is theorized that detritus is composed of the insoluble fractions of humic materials, although it also arise from the decomposition of the phytoplankton (Kirk, 1994). The photosynthetic pigments of phytoplankton are the fourth component responsible for absorption of light in aquatic ecosystems. Absorption of light by phytoplankton cells is the major factor determining the reflectance signal from seawater, whose spectral variations are used in remote sensing to estimate their biomass in the oceans (García *et al.*, 1998). Phytoplankton has absorption peaks in the blue and red portions of the spectrum, due to the presence of their principal pigment, Chlorophyll-a (Chl-a). Smaller peaks in absorption at other wavelengths occur, depending on the natural phytoplankton assemblages (and the specific pigment composition in their cells). In general, oceanic waters should exhibit absorption curves dominated by phytoplankton while coastal waters have a large contribution of CDOM and detritus absorption, specially in waters with high river influence.

Scattering occurs when a photon interacts with some component of the medium in such a way that it is caused to diverge from its original path (Kirk, 1994). Scattering itself does not remove light from the system, a scattered photon still being available for photosynthesis. The effect of scattering is to impede the vertical penetration of light. As a photon is scattered, the probability that it is captured by one of the absorbing components of the medium increases. Some photons are actually scattered back in an upward direction, this property is known as backscattering. The ratio between backscattering and absorption yields the remote sensing reflectance, an important measurement for estimating Chl-a values from space. Scattering is caused in natural waters by molecular scattering of water itself and particles, including phytoplankton. Water scatters light inversely with the fourth power of the wavelength (Kirk, 1994). The angular distribution of light scattered by water is the same in the forward and backward directions (Kirk, 1994). The lowest value for scattering in natural waters is 10 times as high as the value for pure water at that wavelength. Total light scattering in natural waters is dominated by the particle contribution and increases broadly in proportion of the concentration of suspended particulate matter. In coastal waters, scattering is much higher due to the presence of resuspended particles, river-borne terrigenous particulate material and phytoplankton. Resuspension of particles is caused by wave action, tidal currents and storms (Kirk, 1994). Phytoplankton can also make a significant contribution to the scattering of light, but their scattering properties vary widely from one species to another (Kirk, 1994). Due to their low refractive index relative to water, phytoplankton cells are weak backward scatterers compared to inorganic particles (Kirk, 1994).

The bio-optical properties can give us information about ecological processes. Given the growing concern of anthropogenic modification of coastal waters and related global changes affecting phytoplankton growth in such waters,

the long term variability and trends of Chl-a have become of major interest. Optical monitoring of coastal waters may be a cost effective and efficient tool for assessing seasonal and regional variations in phytoplankton abundance and bloom dynamics (Li and Smayda, 1998). A better understanding of how light interacts with coastal waters can also help us to explain how phytoplankton populations adapt to seasonal variations in available radiation.

Of all the factors which limit primary production, light is the one that shows the more extreme variation (Kirk, 1994). Spectral quality of light in the sea is susceptible to changes with depth, water transparency, and the nature of the incident solar radiation (Figueiras and Arbones, 1999). In response to the variability in intensity and spectral distribution of available light for photosynthesis in the aquatic ecosystem, phytoplankton has developed physiological adaptations to ensure their survival. The light harvesting capacity of a phytoplankton cell depends in part on the particular combination of photosynthetic pigments present in their thylakoids (Platt, 1981). There are three chemically distinct families of pigments; the chlorophylls, the carotenoids and the biliproteins. Pigments within these families, have different absorption peaks. Chl-a is the most abundant and important of these pigments. Energy is captured by accessory pigments and passed to Chl-a to be used for photosynthesis. Although a given phytoplankton group has a fixed number of pigments specific to that species, it can change the ratio in which these pigments are concentrated in the cell, thus effectively changing the absorption spectrum of that cell (Platt, 1981). It is generally found that as light intensity during growth decrease, the concentration of photosynthetic pigments in the cells increases. Increases in pigment concentration of up to five- fold are commonly observed (Kirk, 1994). These increases are not only in Chl-a, but also in accessory pigments, which can be greater. The increase of photosynthetic pigments that occur as the light

intensity diminishes can be due to an increase in the number of photosynthetic units, or in the average size of the photosynthetic unit, or both.

Other factor that affects the absorption spectrum of a phytoplankton cell is the “package effect”. It occurs because pigment molecules are contained in discrete packages; within chloroplasts, and cells. This diminishes the efficiency at which they collect light from the prevailing field, lowering their specific absorption (Kirk, 1994). Package effect is proportionately greatest when absorption is strongest, flattening the absorption peaks. This effect is regulated by the size and shape of phytoplankton cells. As a general rule, the larger the cells, the less efficient is the light capture process. Elongated cell shapes, in the other hand, tend to absorb more light than spherical shapes.

## INTRODUCTION

Coastal waters are known for their large variability in optical properties (Kirk, 1994). This is the result of a complex and dynamic array of processes that operates in these systems. The interaction of these processes, both in a temporal and spatial scale, causes variation in the abiotic and biotic components of the water column, which affect its optical characteristics. Assessing the range and sources of this variability is important for the development of remote sensing algorithms capable of accurately measuring Chl-a. Establishing regional algorithms for calculating Chl-a concentration from satellite data is required to obtain proper estimates of phytoplankton biomass and primary production (García et. al., 1998).

In most marine areas, absorption and backscattering coefficients of phytoplankton are fundamental variables controlling optical properties (Morel, 1987). Absorption of light by phytoplankton cells is the major factor determining the reflectance signal from seawater (Gordon and Morel, 1983). These bio-optical properties, when combined with ancillary data, can be used to study phytoplankton ecology.

Historically, it has been difficult to obtain a full data set of optical parameters in a short time span (i.e. a day), due to lack of technology to perform these measurements in the field (e.g. backscattering), and the geographical extension needed to navigate in order to locate contrasting optical provinces. Modern instrumentation has made possible the collection of *in situ* data sets of optical parameters such as particulate absorption ( $a_p$ ), CDOM ( $a_g$ ), backscattering coefficient ( $b_b$ ), remote sensing reflectance ( $R_{rs}$ ), and Chl-a concentration on space and time scales previously impossible to sample. This information can be used to assess the relative importance of specific optical constituents in a particular system.

Puerto Rico offers a good opportunity to study optical properties in tropical coastal waters. In the tropics, the seasonal rainfall patterns produce clear changes in river discharge. Changes in both the amount and the biogeochemical nature of river discharge occur through the year due to large variations in climatic and topographic conditions combined with anthropogenic factors (Gilbes *et al.*, 1996). These sources of variation, affect important oceanic parameters such as salinity, nutrient concentration, light attenuation, and suspended sediments, thus affecting bio-optical properties.

Mayagüez Bay is an excellent natural laboratory to study optical properties. Located in the west coast of Puerto Rico, it is subjected to the influence of three major rivers. The Añasco, Yagüez and Guanajibo rivers supply a considerable load of terrigenous sediments, especially during the rainy season, extending from September through November. According to Morelock *et al.* (1983), the Añasco- Mayagüez basin receives an average precipitation range of 200 - 250 cm per year. The mean discharge of these rivers during 1997-1998 varied from  $2.21 \text{ m}^3\text{s}^{-1}$  to  $13.55 \text{ m}^3\text{s}^{-1}$  for Añasco River and  $0.71 \text{ m}^3\text{s}^{-1}$  to  $13.85 \text{ m}^3\text{s}^{-1}$  for the Guanajibo River (US Geological Survey, 1998). The Añasco River is the largest river of the west coast, and although its basin was used for agriculture in the past, nowadays is much more developed. The Yagüez basin is highly developed and highly influenced by anthropogenic activities. The Guanajibo basin was traditionally dedicated to agriculture, especially to the sugar cane industry, but it is not being cultivated actively in the present. Beside these rivers, a number of smaller streams discharge to the bay.

The location of tuna processing facilities close to the Yagüez River mouth is another source of nutrients and particulate matter to the bay. These industries dump waste waters into the bay on a regular basis. Mayagüez Bay is also subjected to sewage waters input. The Puerto Rico Waters Authority discharges

primary treated water from the city sewer systems through a diffuser tube located between the Añasco River mouth and the tuna factories. Both the riverine and the anthropogenic inputs to the bay supply nutrients and suspended particles to the system. All these interactions may suggest the existence of several bio-optical provinces in a relatively small area.

## **OBJECTIVES**

The main objective of this work is to characterize the spatial and temporal variability of inherent and apparent optical properties in Mayagüez Bay. A secondary objective is to study how this variability is regulated by the abiotic and biotic factors in the system. The analysis of how these variables are related may provide a better understanding of the behavior of phytoplankton assemblages in Mayagüez Bay. The hypotheses considered in this work are:

1. Bio-optical properties in Mayagüez Bay are highly variable and influenced mostly by rainy and dry seasonal patterns.
2. Correlation exist between river discharge and absorption, backscattering and reflectance measurements in the bay.
3. Light is the limiting factor for phytoplankton populations during the rainy season.

## METHODS

### *Field Work*

Six stations were routinely sampled at Mayagüez Bay (Figure 1) to evaluate the influence of the seasonal river discharge and industrial effluents on the bio-optical properties. Monthly samples were collected from February 1997 to January 1998. At each station, water samples were taken from the surface for Chl-a concentration, absorption measurements and nutrient analysis. Temperature and salinity profiles were obtained at each station using a SBE-19 CTD from Sea-Bird Electronics. Profiles of the backscattering coefficient ( $b_b$ ) at six wavelengths were obtained using the Hydroscat-6 (from Hobi Labs). Water radiance,  $L_0(\lambda)$ , sky radiance,  $L_s(\lambda)$ , and the above surface downwelling irradiance,  $E_d(0^+, \lambda)$  were measured using a GER 1500 portable spectroradiometer.  $L_0(\lambda)$  was measured aiming the GER 45° to the vertical into the water surface, maintaining an azimuth of 90° from the solar plane to minimize sun glint.  $L_s(\lambda)$ , was measured pointing the GER 45° to the vertical to the sky, maintaining an azimuth of 90° from the solar plane.  $E_d(0^+, \lambda)$  was measured pointing directly upward using a cosine collector attached to the GER. The remote sensing reflectance,  $Rrs(\lambda)$ , was calculated using the following equation:

$$Rrs(\lambda) = \frac{L_0(\lambda) - f(L_s(\lambda))}{E_d(0^+, \lambda)}$$

Where  $f$  is the Fresnel's number, the percent of sky radiance reflected back to the atmosphere. Fresnel's number has a value of 0.28 at a 45° angle.

An additional cruise took place in July 1998. All of the above measurements were taken. In addition, samples for measuring the absorption of CDOM were collected. Two more cruises were carried out in October 1999. During the October 19 cruise, six stations were sampled at different distances



Figure 1. Stations sampled during 1997 and 1998 cruises in Mayagüez Bay.

from the Guanajibo River mouth. Samples were also taken for determination of total suspended particulate matter concentrations. On October 24, five stations were sampled approaching the Yagüez River mouth (Figure 2). In this cruise an optical package containing an AC-9 (Wet Labs), a SBE-19 CTD, a WetStar fluorometer (Wet Labs), and a OCR-200 Profiling radiometer (Satlantic) was deployed.

#### *Laboratory work*

Water samples were filtered *in situ* using the filter pad technique proposed by Mitchell and Kieffer (1984). The samples were collected on 25 mm Whatman GF/F filters. These filters were kept at 0°C until absorption measurements were done. The absorption spectra between 375 and 800 nm was measured using a GER 1500 portable spectroradiometer attached to a Licor integrating sphere through a fiber optic cable. A blank filter was made passing a volume of 200 milliliters of distilled water. The absorption of the blank was also measured and the difference between the sample and the blank spectra was taken as the particulate absorption spectrum ( $a_p$ ). Following this measure, hot methanol was passed through the filter (Kishino *et al.*, 1985), and the measurement procedure repeated. These spectra were taken as absorption by non-methanol extractable detrital material ( $a_d$ ). The difference between  $a_p$  and  $a_d$  represents the phytoplankton absorption ( $a_{ph}$ ). This value, divided by the Chl-a concentration correspond to the Chlorophyll-a specific absorption coefficient ( $a_{ph}^*$ ). All spectra were shifted to zero absorbance at 750 nm and corrected for pathlength amplification using the  $\beta$  factor from Bricaud and Stramsky (1990). Chl-a concentration extracted in methanol was measured with a Turner Designs Model 10-AU fluorometer using the method developed by Welschmeyer (1994). This

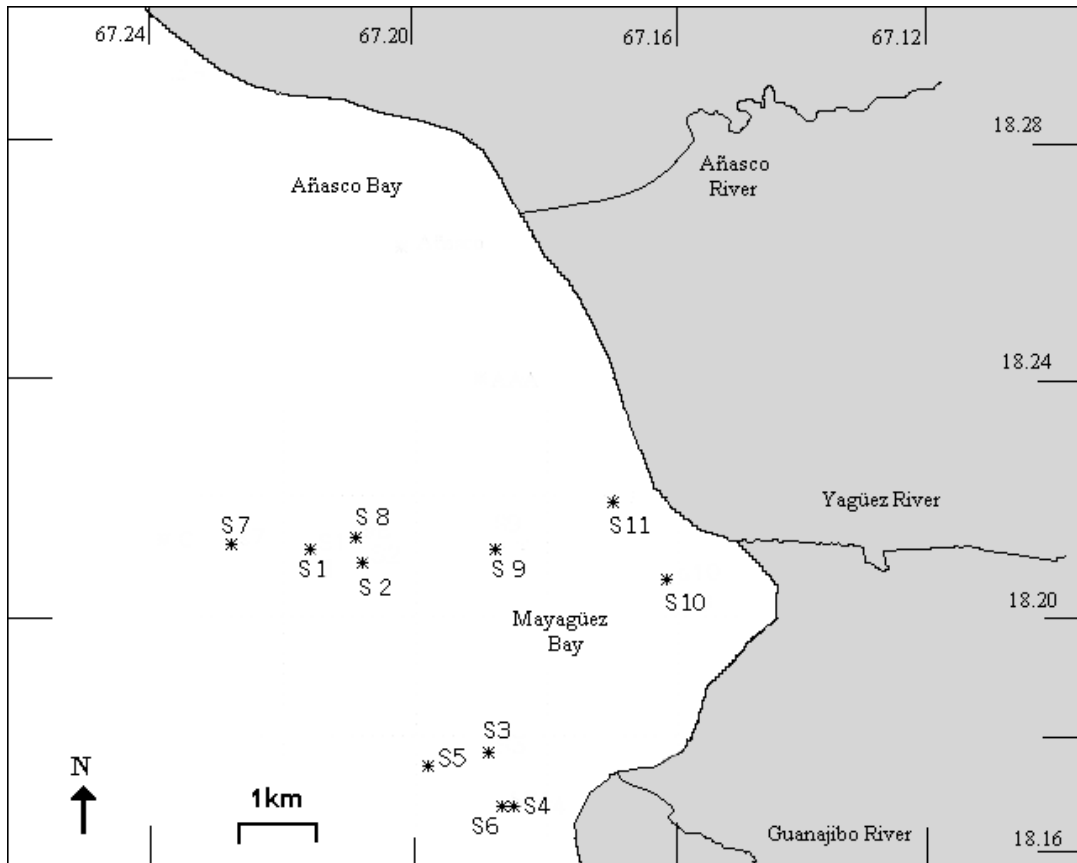


Figure 2. Stations sampled on October, 1998. Stations 1 to 6 were sampled on October 19 and Stations 7 to 11 on October 24.

set-up provides the capacity of measuring the Chl-a concentration directly, without acidification of the sample. The fluorometer was calibrated using Chl-a from the alga *Anacystis nidulans*.

CDOM samples were obtained using only materials made of crystal and Teflon. All materials were thoroughly cleaned with 1M HCl and 1M NaOH solutions, and rinsed with distilled water. Crystalware and filters were combusted for at least 6 hours at 300°C to remove any trace of organic matter. Absorption spectra of CDOM ( $a_g$ ) were obtained filtering seawater through a pre-combusted GF/F filter and collecting the filtrate in amber glass bottles. The absorbances of the samples were measured from 250 to 750 nm in a Pelkin Elmer Lambda 18 dual beam spectrophotometer following the suggestions of Bricaud *et al.* (1981).

The concentration of total suspended particulate matter (SPM) was measured using Millipore HA 0.45  $\mu\text{m}$  cellulose acetate filters. The filters were desiccated in an oven for 24 hours at 70-80°C. The weight of each filter was recorded to five significant figures using a Mettler analytical balance. Filters were stored in a glass dessicator with silica gel until use. A known volume of seawater was filtered and the filters were desiccated in the oven again to remove the water before weighing for second time. The difference between the filter weight before and after filtration was taken as the SPM ( $\text{mg l}^{-1}$ ).

#### *Data analysis*

Two-way analyses of variance (ANOVA) were used to evaluate the temporal and spatial variability of  $a_p$ ,  $a_d$ ,  $a_{ph}$  and  $a_{ph}^*$ . The analyzed wavelengths correspond to those found in the Sea-viewing Wide Field-of-view Sensor (SeaWiFS), namely 412, 443, 490, 510, 555 and 670 nm. The data were analyzed using the  $\log_{10}$  transformation to normalize it. Similar calculations were done with  $b_b$ ,  $a_g$ , and  $R_{rs}$ , trying to establish the sources of variation from both the

ANOVA results and graphic examination of the data. Correlation analysis were performed between several optical variables, Chl-a and river discharge. The CDOM spectral slopes were calculated from linear-least-square regressions of the plot of  $\ln a_g(\lambda)$  vs. wavelength for the interval between 412 and 443 nm. This interval was chosen because CDOM absorption is greater there and those wavelengths have been suggested to discriminate between Chl-a and CDOM in future bio-optical algorithms.

## RESULTS

### *Inherent Optical Properties*

Figure 3 illustrates some examples of the absorption curves obtained at Mayagüez Bay from February 1997 to January 1998. The spatial variability of total particulate absorption,  $a_p$ , was highly significant ( $p < 0.001$ ) at the six analyzed wavelengths. The  $a_p$  also showed significant temporal differences at those wavelengths, except for 555 nm. The highest particulate absorption values were found during October 1997 in Añasco station, and the lowest values were found during March 1997 in Manchas station. This pattern is shown in the six analyzed wavelengths. The Añasco station also showed the greatest range in  $a_p$  values during this study (Figure 4). Correlations made between  $a_p$  at 443, 555, 670 nm and Chl-a did not reveal any strong relationship. In general,  $a_p$  was highest in Añasco station and lowest in Oceánica station through time. April, August, and October were the months with the highest  $a_p$  values.

Detritus absorption ( $a_d$ ) followed a similar trend to particulate absorption. It was highly significant in space ( $p < 0.001$ ) but it did not show temporal differences except for 412 and 443 nm ( $P < 0.01$  and  $P < 0.05$ , respectively). The highest  $a_d$  value was found at Añasco station during October 1997 and the lowest  $a_d$  value was found in Oceánica station during June 1997 (Figure 5).

Phytoplankton absorption,  $a_{ph}$ , was also highly variable in space, showing significant differences at all the examined wavelengths ( $P < 0.001$ ). At the temporal level  $a_{ph}$  showed significant differences in all analyzed wavelengths except at 443 nm. The maximum  $a_{ph}$  value was at Añasco station during November 1997 and the minimum value was at Manchas during September 1997.

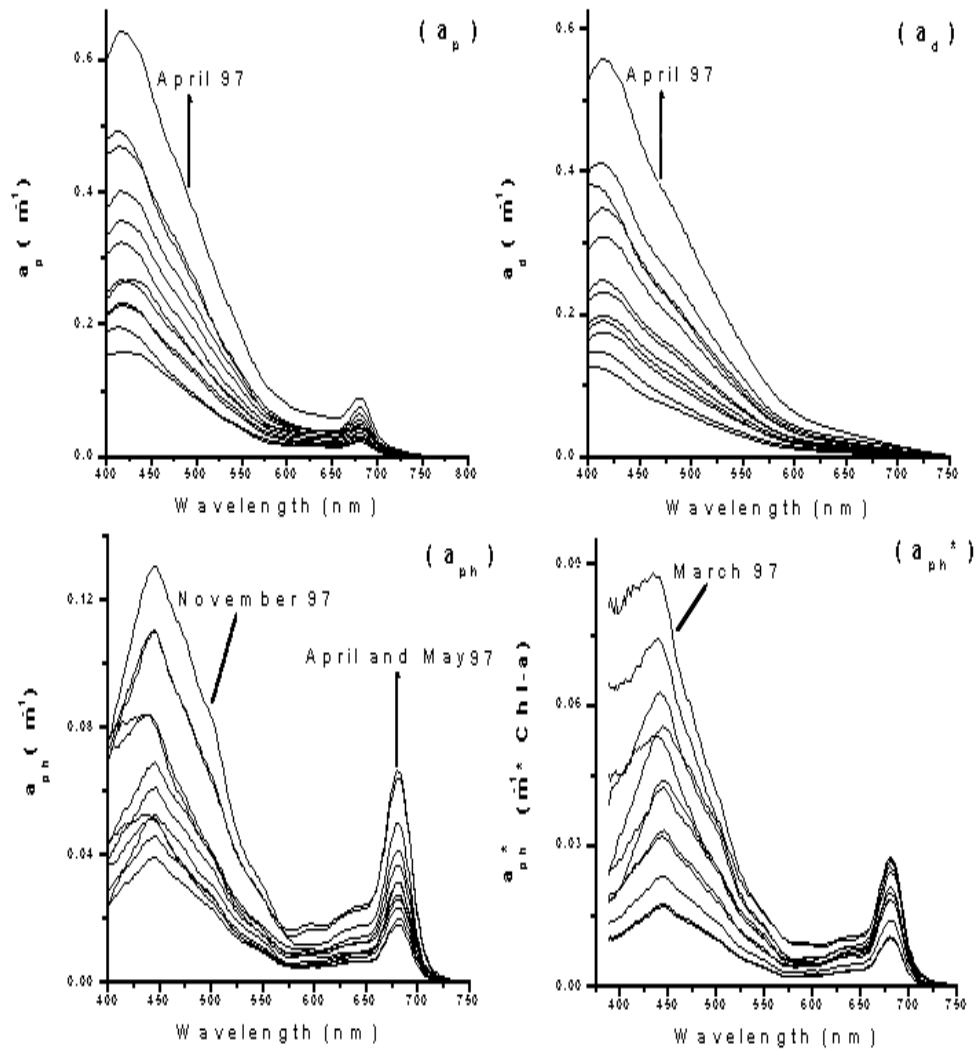


Figure 3. Absorption coefficients at surface for Atuneras station from February 1997 to January 1998.

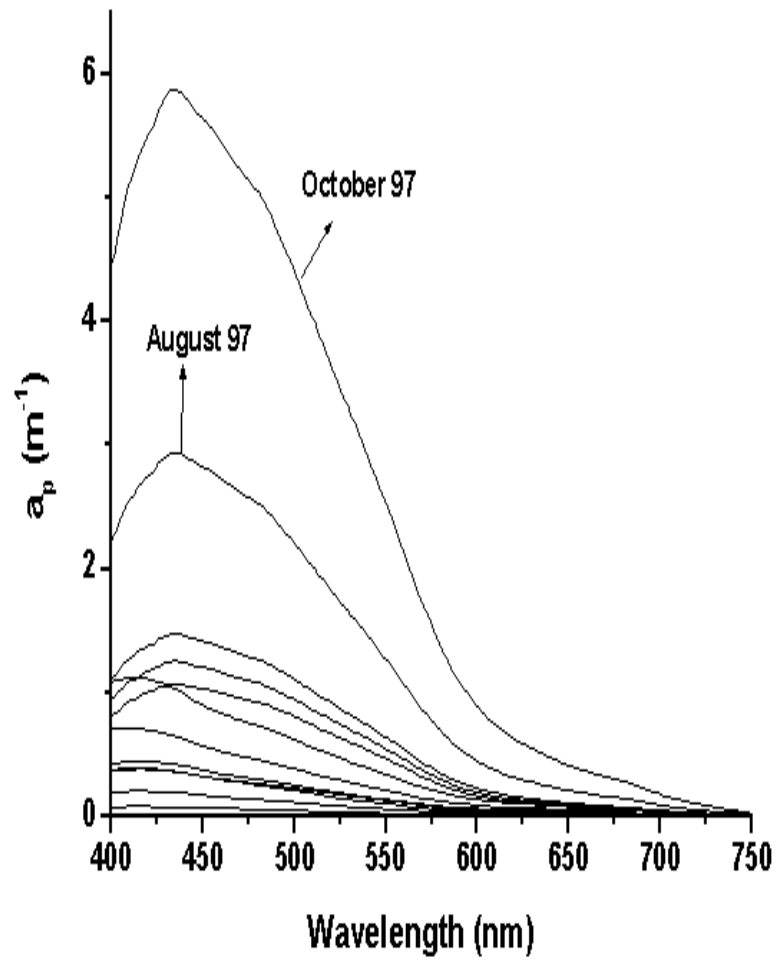


Figure 4. Particulate absorption coefficient ( $a_p$ ) at surface in Añasco station from February 1997 to January 1998.

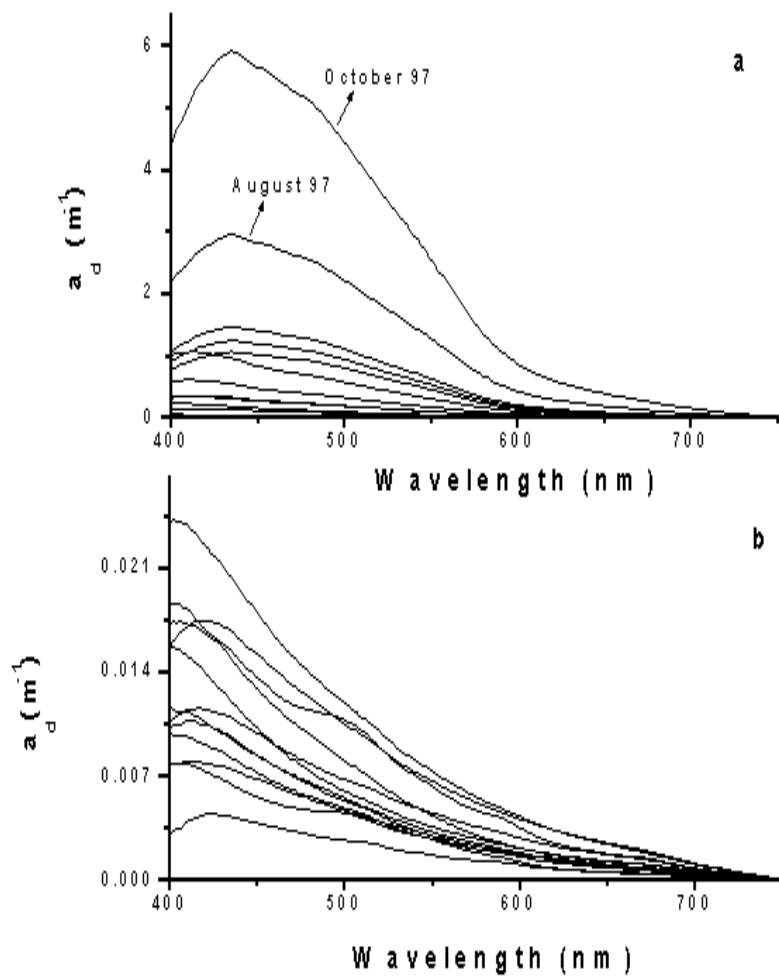


Figure 5. Detritus absorption coefficient ( $a_d$ ) at surface in Añasco station (a) and Oceánica station (b) from February 97 to January 98.

Note that although the highest  $a_{ph}$  value was recorded in Añasco station, the three values following the lowest value were recorded in that station as well.

The specific absorption coefficient of phytoplankton ( $a_{ph}^*$ ) was significantly different in space only at 412 and 443 nm ( $P < 0.05$ ), but it was significantly different in time at all wavelengths except for 670 nm. The maximum value was at Añasco station during February 1997 and the minimum value was at Añasco station during April 1997. A summary of the results for all the absorption analyses is presented in Table 1.

In July 1998, the highest  $a_p$  were detected in Añasco station ( $0.73 \text{ m}^{-1}$  at 412 nm). The lowest were in Oceánica and Rodríguez stations ( $0.061 \text{ m}^{-1}$  at 412 nm). Añasco station also showed the highest  $a_d$  ( $0.68 \text{ m}^{-1}$  at 412 nm) and Oceánica and Rodríguez stations showed the lowest ( $0.030 \text{ m}^{-1}$  at 412 nm). The  $a_{ph}$  were the highest in Atuneras and Acueductos stations ( $0.20 \text{ m}^{-1}$  and  $0.16 \text{ m}^{-1}$  at 443 nm, respectively) and the lowest in Oceánica and Rodríguez stations ( $0.036 \text{ m}^{-1}$  and  $0.040 \text{ m}^{-1}$  at 443 nm, respectively). The  $a_{ph}^*$  were the highest in Manchas station ( $0.06$  at 443nm) and Oceánica station ( $0.059 \text{ m}^{-1}$  at 443 nm). The lowest values were recorded in Atuneras station ( $0.034 \text{ m}^{-1}$  at 443 nm). These results are presented in Figure 6. The highest  $a_g$  was found in Añasco station with  $0.43 \text{ m}^{-1}$  at 412 nm. Other stations had values ranging from 0.17 to  $0.10 \text{ m}^{-1}$  at 412 nm. These data are shown in Figure 7. The spectral slopes of  $a_g$  curves are shown in Table 2.

In October 1999, stations 1 to 6 (Figure 2) showed an increase in  $a_p$  as the station approached to the Guanajibo River mouth. As  $a_p$  increases  $a_d$  increases accordingly. There is also an increase in  $a_{ph}$ , although it is a much smaller fraction of  $a_p$  in the stations close to the mouth. Figure 8 demonstrates these trends. The  $a_{ph}^*$  shows large variability at 443 nm and lower variability at 670 nm. Stations 8 to 11 (Figure 2) show a similar pattern to the Guanajibo stations.

Table 1. Analysis of Variance (two-way, without replicates) between stations and months for the absorption coefficients (S. = Significant, N.S = Non significant). P equals probability of no statistically significant differences.

Parameter	Significance in Space	P	Significance in Time	P
a <sub>p</sub> 412	S.	<0.001	S.	<0.01
a <sub>p</sub> 443	S.	<0.001	S.	<0.05
a <sub>p</sub> 490	S.	<0.001	S.	<0.05
a <sub>p</sub> 510	S.	<0.001	S.	<0.05
a <sub>p</sub> 555	S.	<0.001	N.S.	N.S.
a <sub>p</sub> 670	S.	<0.001	S.	<0.01
a <sub>d</sub> 412	S.	<0.001	S.	<0.01
a <sub>d</sub> 443	S.	<0.001	S.	<0.05
a <sub>d</sub> 490	S.	<0.001	N.S.	N.S.
a <sub>d</sub> 510	S.	<0.001	N.S.	N.S.
a <sub>d</sub> 555	S.	<0.001	N.S.	N.S.
a <sub>d</sub> 670	S.	<0.001	N.S.	N.S.
a <sub>ph</sub> 412	S.	<0.001	S.	<0.01
a <sub>ph</sub> 443	S.	<0.001	N.S.	N.S.
a <sub>ph</sub> 490	S.	<0.001	S.	<0.001
a <sub>ph</sub> 510	S.	<0.001	S.	<0.01
a <sub>ph</sub> 555	S.	<0.001	S.	<0.001
a <sub>ph</sub> 670	S.	<0.001	S.	<0.001
a <sub>ph</sub> * 412	S.	<0.05	S.	<0.001
a <sub>ph</sub> * 443	S.	<0.05	S.	<0.001
a <sub>ph</sub> * 490	N.S.	N.S.	S.	<0.05
a <sub>ph</sub> * 510	N.S.	N.S.	S.	<0.01
a <sub>ph</sub> * 555	N.S.	N.S.	S.	<0.001
a <sub>ph</sub> * 670	N.S.	N.S.	N.S.	N.S.

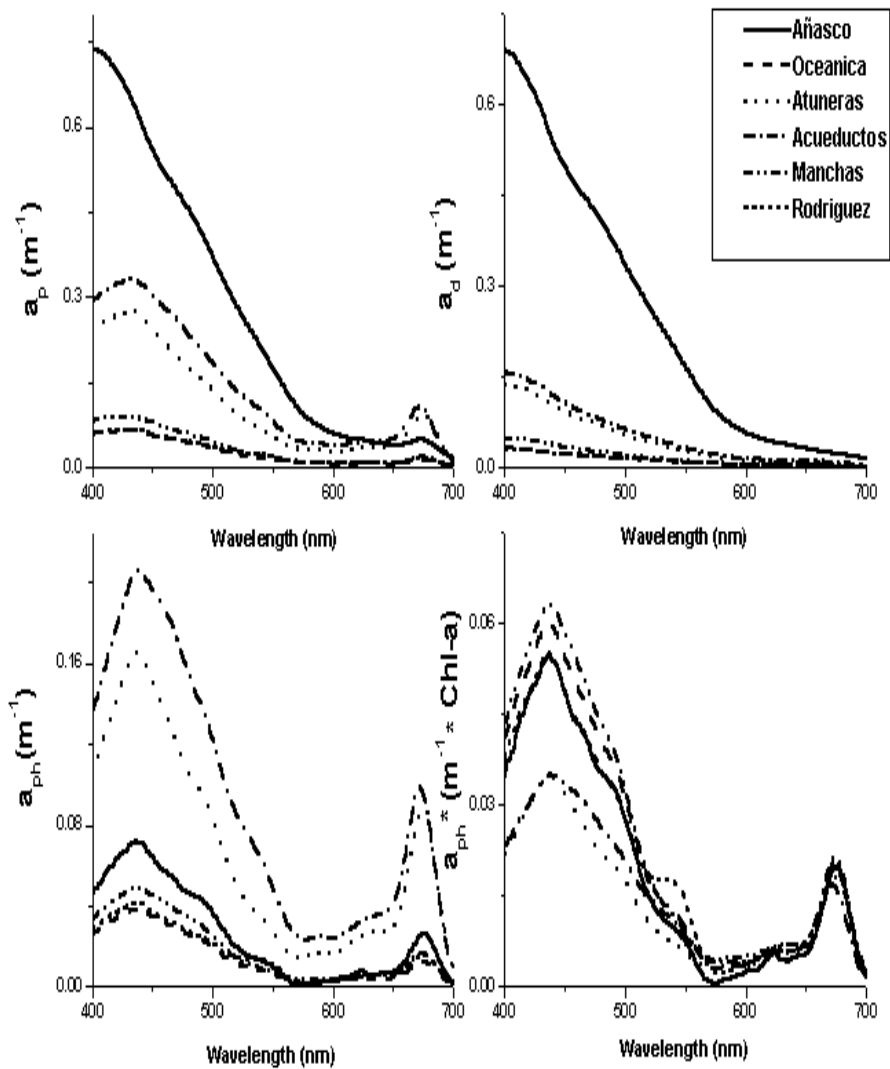


Figure 6. Spectra of  $a_p$ ,  $a_d$ ,  $a_{ph}$  and  $a_{ph}^*$  in Mayagüez Bay during July 98. The legend at the top right corner applies to all graphs.

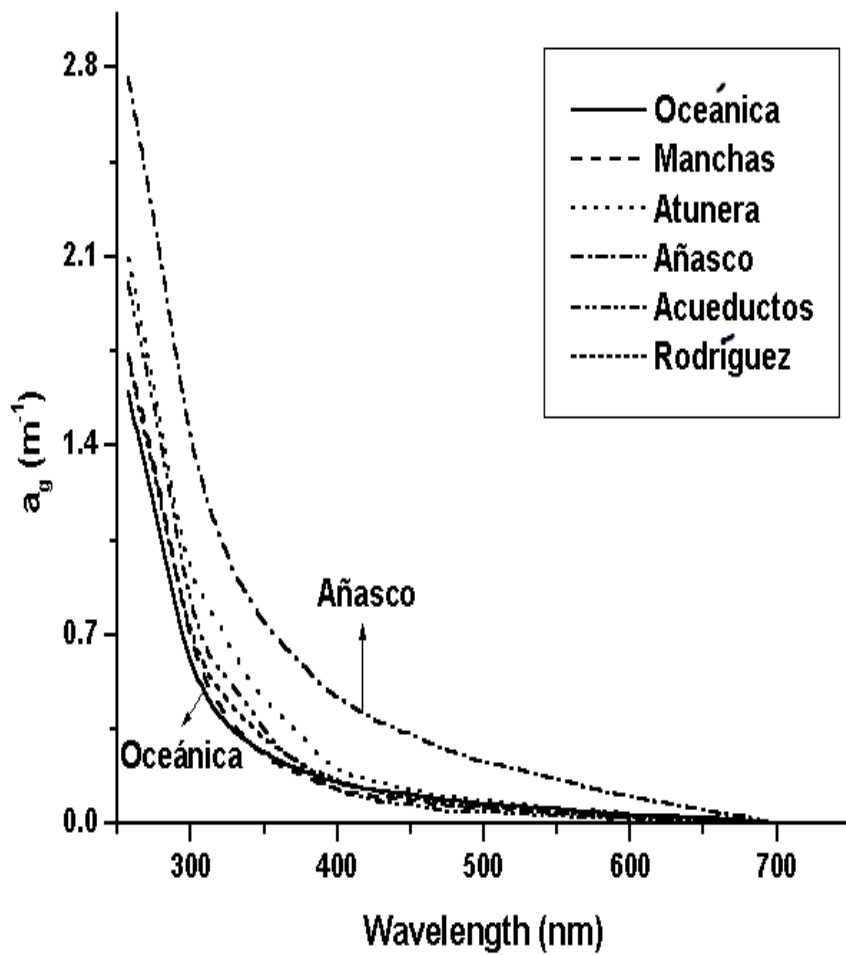


Figure 7. Spectra of  $a_g$  in Mayagüez Bay during July 1998.

Table 2. Absorption coefficients of CDOM ( $a_g$ ) at 412 and 443 nm and spectral slopes during July 98 and October 99.

<b>Sample</b>	<b>Date</b>	<b><math>a_g</math> 412 nm</b>	<b><math>a_g</math> 443 nm</b>	<b>Spectral Slopes</b>
Oceánica	July 98	0.2308	0.1823	0.00732
Manchas	July 98	0.1159	0.0900	0.00781
Atuneras	July 98	0.1772	0.1338	0.00915
Añasco	July 98	0.4286	0.3445	0.00695
Acueductos	July 98	0.1910	0.1397	0.00989
Rodríguez	July 98	0.1416	0.1031	0.00958
station 1	October 99	0.1249	0.0908	0.0103
station 2	October 99	0.1727	0.1160	0.0129
station 3	October 99	0.4498	0.3083	0.0122
station 4	October 99	2.3819	1.4989	0.0149
station 5	October 99	0.3281	0.2229	0.0124
station 6	October 99	0.5656	0.3746	0.0132
station 7	October 99	0.1209	0.0880	0.0103
station 8	October 99	0.1810	0.1330	0.0099
station 9	October 99	0.6277	0.4632	0.0098
station 10	October 99	1.0550	0.6471	0.0158
station 11	October 99	0.8853	0.5774	0.0138
<b>Mean</b>		0.4811	0.3243	0.0110
<b>Std. Dev.</b>		0.5641	0.3505	0.0026
<b>Min.</b>		0.1159	0.0880	0.0070
<b>Max.</b>		2.3819	1.4989	0.0158

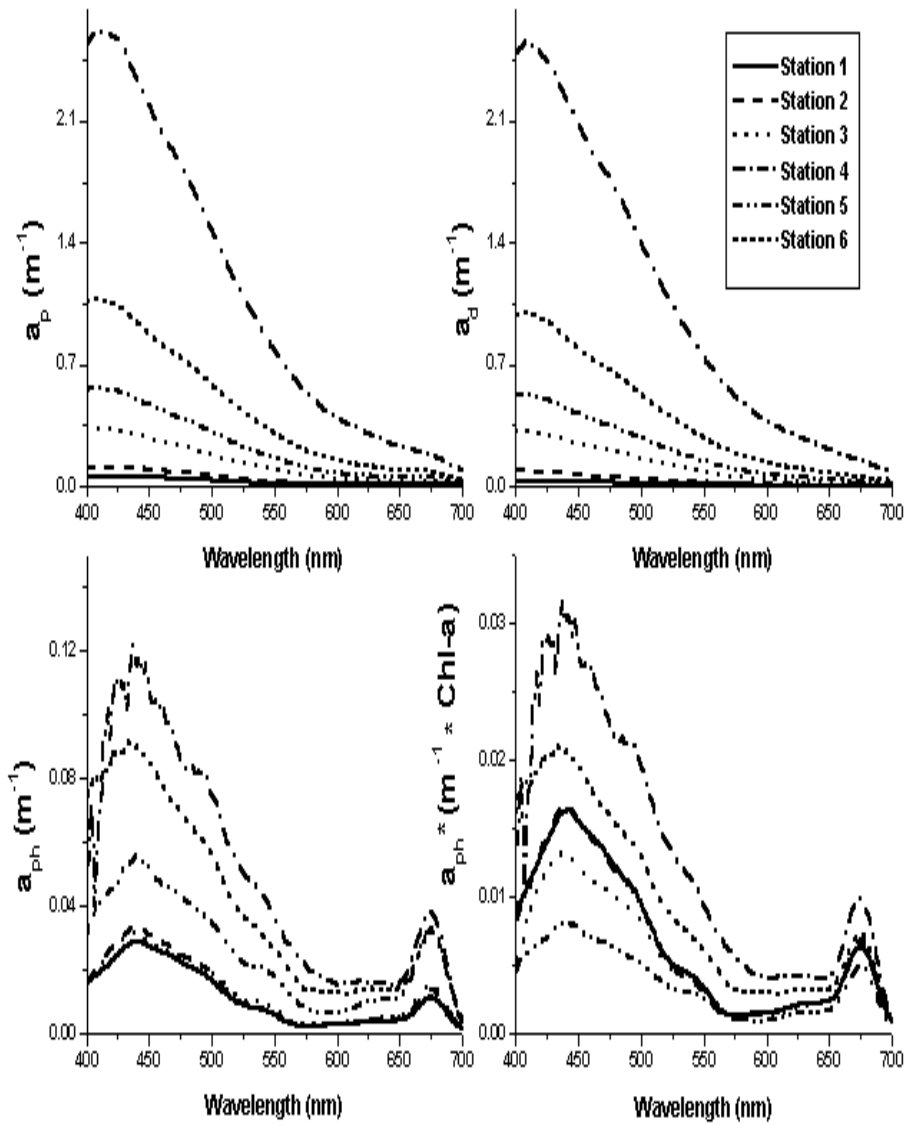


Figure 8. Spectra of  $a_p$ ,  $a_d$ ,  $a_{ph}$  and  $a_{ph}^*$  for stations 1 to 6 during October 1999. The legend at the top right corner applies to all graphs.

An increase in  $a_p$ ,  $a_d$  and  $a_{ph}$  was found as the station gets closer to the Yagüez River mouth (Figure 9). The  $a_{ph}$  shows a great range of variability at the 443 nm peak but lower variability at the 670 nm peak (Figure 9). The  $a_g$  showed the highest values in stations closer to the river mouth, namely station 4 and Station 10 (Figure 10). In station 4, the maximum value was  $2.38 \text{ m}^{-1}$  at 412 nm. A maximum value of  $1.06 \text{ m}^{-1}$  at 412 nm was observed at station 10.

Backscattering coefficients from November 1997 to January 1998 for Atuneras and Añasco stations are shown in Figure 11. These data showed significant spatial differences ( $P < 0.001$  to  $P < 0.01$ ) in the six channels of the Hydrosat-6, (442, 470, 510, 589, 620 and 671 nm). Significant temporal differences ( $P < 0.01$  to  $P < 0.05$ ) were also found at most wavelengths except at 589 nm. Maximum values were found in December 1997 at the Atuneras station, and minimum values were found at the Oceánica station in January 1998. Atuneras station had the highest  $b_b$  values through the year, followed by Añasco and Acueductos, the smallest values were recorded at the Oceánica station. The profiles showed a tendency of decreasing  $b_b$  with increasing wavelength. This pattern is not observed in the red wavelengths (620 and 671 nm) as shown in Figure 12. The  $b_b$  and  $a_p$  revealed a strong positive correlation at the three pairs of analyzed wavelengths (442 x 443, 589 x 555 and 671 x 670 nm) (Figure 13). The correlation between  $b_b$  (671) and  $a_p$  (670) was specially strong with a correlation coefficient of 0.93,  $n=17$ . A linear regression curve fitted to the data yielded a regression coefficient of 0.86. The backscattering coefficient and Secchi depth revealed moderately strong negative correlations. The data were fitted with a power regression equation which resulted in high regression coefficients. These results are summarized in Table 3 and Table 4. Backscattering values for July 1998 are shown in Figure 14. The data shows the highest backscattering values

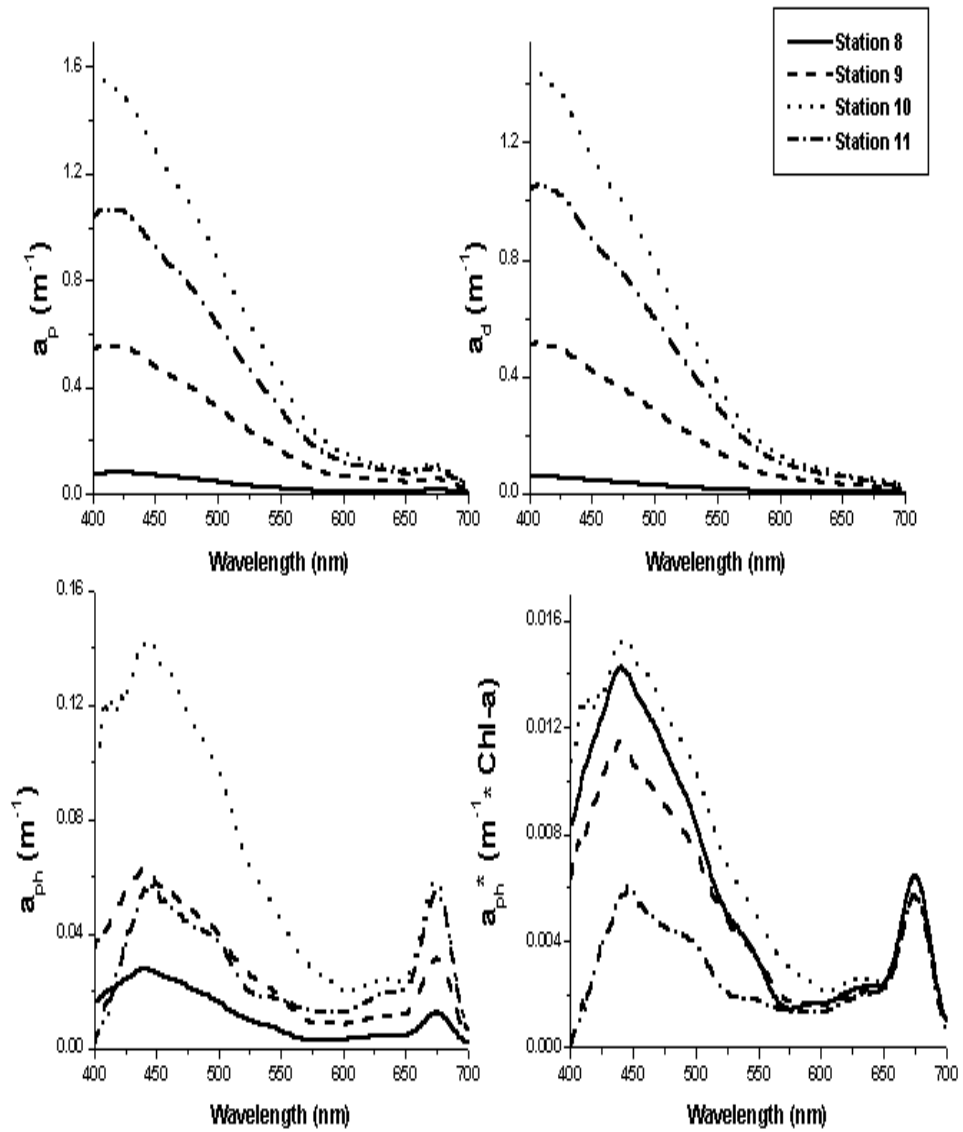


Figure 9. Spectra of  $a_p$ ,  $a_d$ ,  $a_{ph}$  and  $a_{ph}^*$  for stations 8 to 11 during October 1999. The legend at the top right corner applies to all graphs.

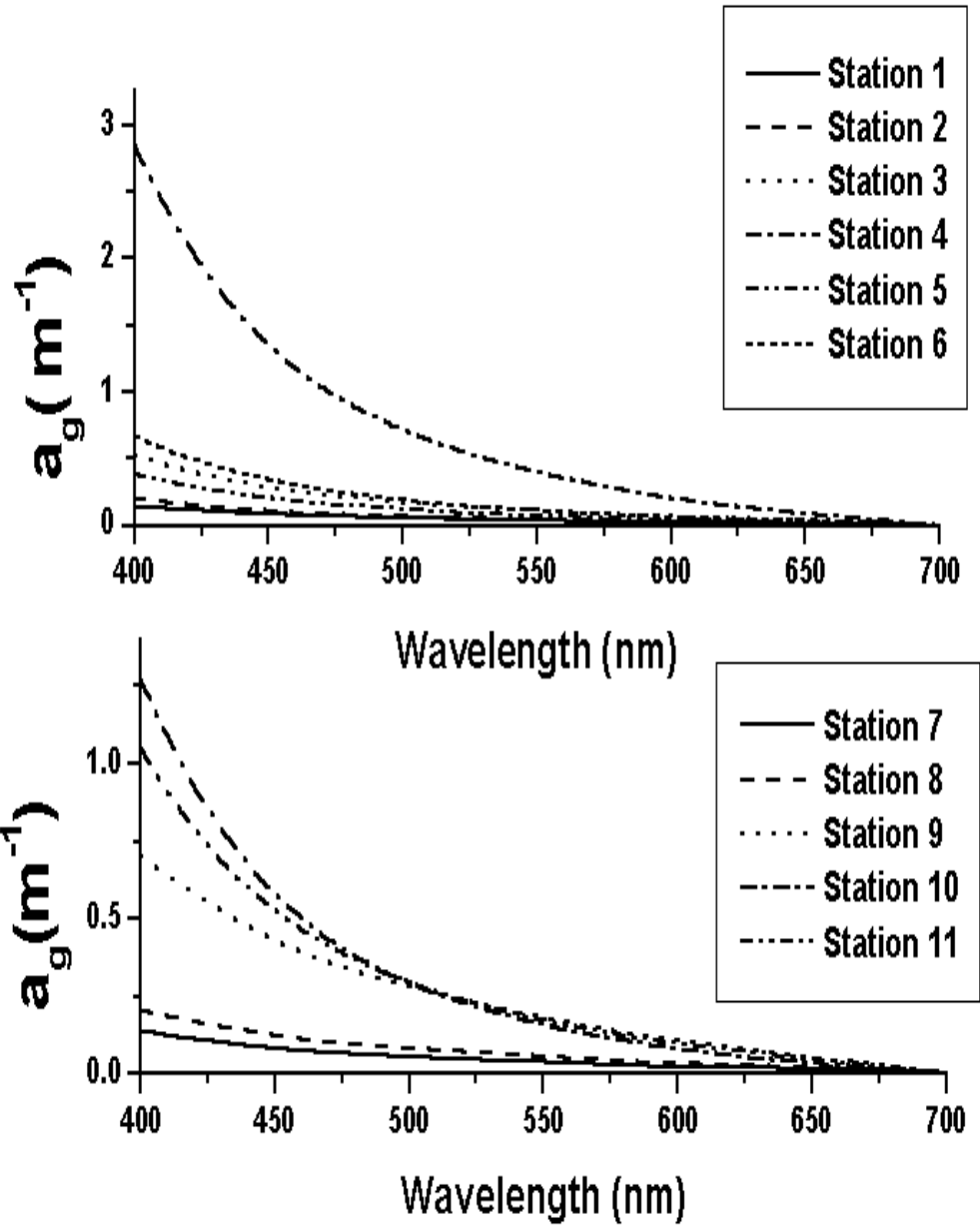


Figure 10. Spectra of  $a_g$  in Mayagüez Bay during October 99.

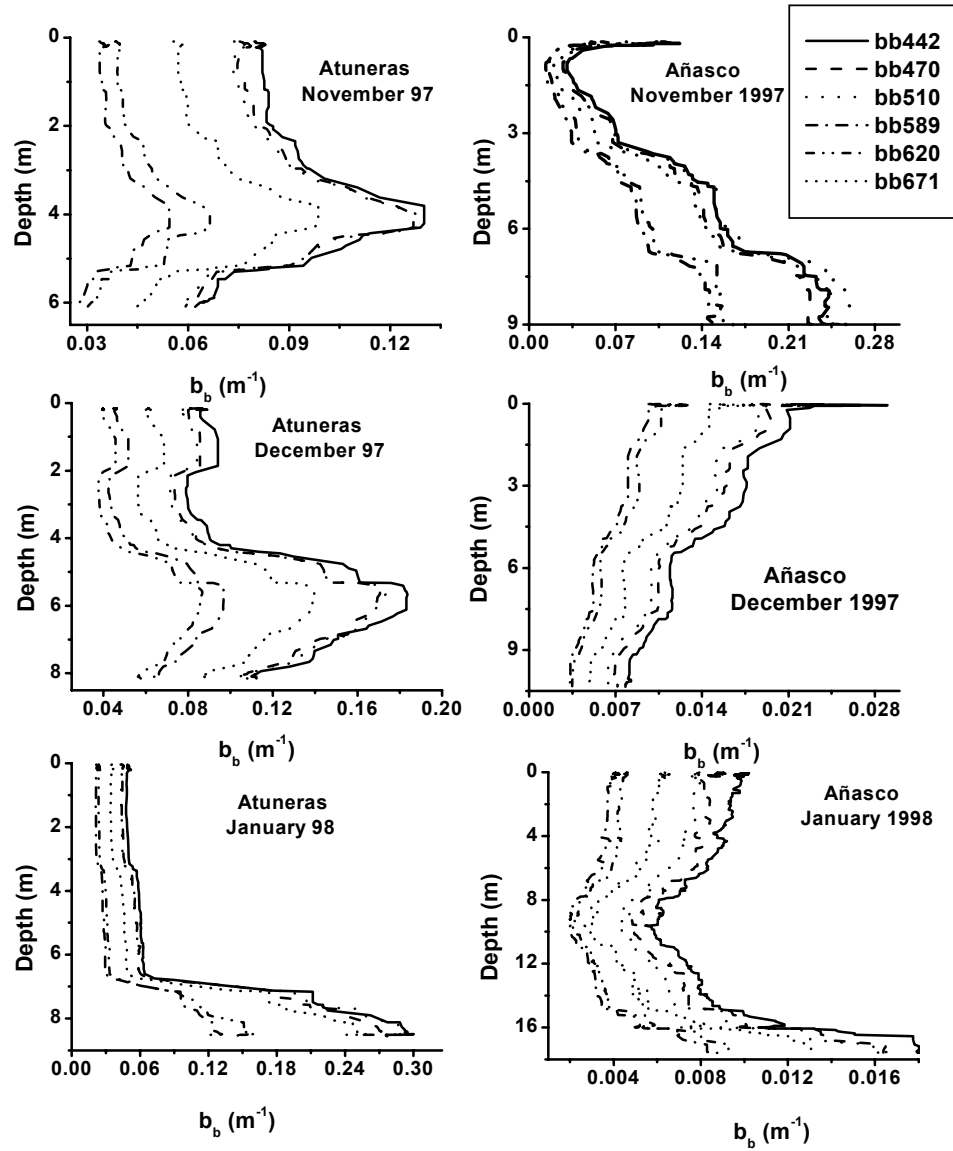


Figure 11. Profiles of the backscattering coefficient for Atuneras and Añasco stations for November 1997 (top), December 1998 (middle) and January 1998 (bottom). The legend at the top right corner applies to all graphs.

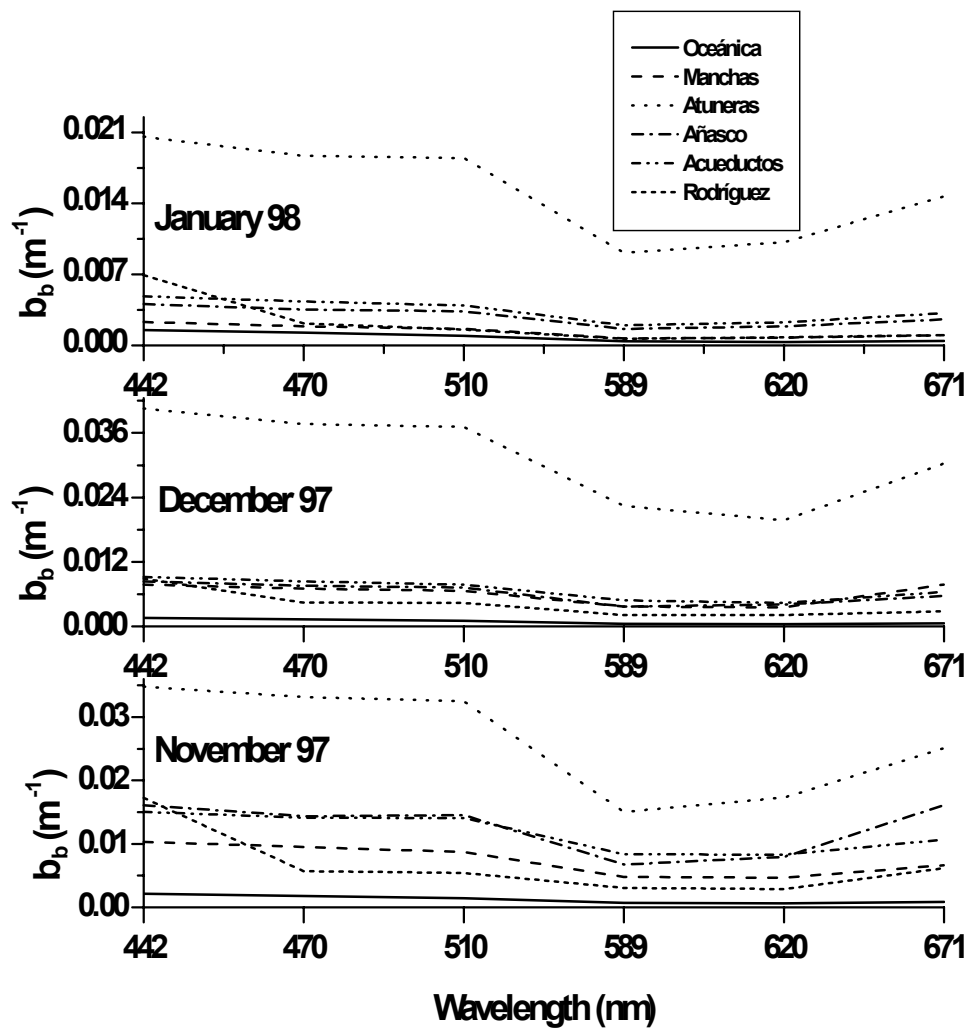


Figure 12. Relationship of  $b_b$  and wavelengths measured in Mayagüez Bay from November 1997 to January 1998. Legend at the top right corner applies to all graphs.

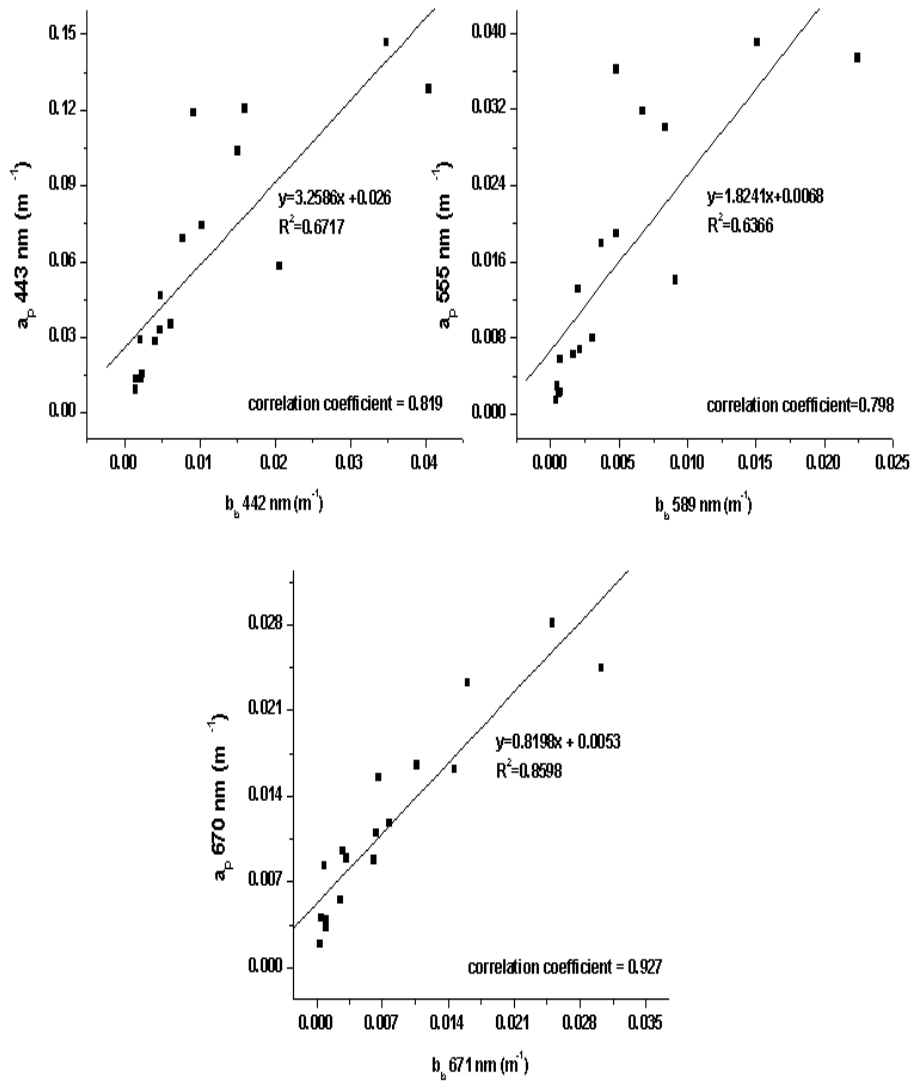


Figure 13. Linear fits and correlation coefficients of  $b_b$  vs.  $a_p$  at the selected wavelengths.

Table 3. Analysis of Variance (two-way, without replicates) between stations and months for the backscattering coefficient (S. = Significant, N.S = Non significant). P equals probability of no statistically significant differences

<b>Parameter</b>	<b>Significance in Space</b>	<b>P</b>	<b>Significance in Time</b>	<b>P</b>
b <sub>b</sub> 442	S.	<0.001	S.	<0.01
b <sub>b</sub> 470	S.	<0.001	S.	<0.05
b <sub>b</sub> 510	S.	<0.001	S.	<0.05
b <sub>b</sub> 589	S.	<0.01	N.S.	N.S.
b <sub>b</sub> 620	S.	<0.001	S.	<0.05
b <sub>b</sub> 671	S.	<0.001	S.	<0.05

Table 4. Correlation between backscattering coefficient and selected parameters.

<b>Parameters</b>	<b>Correlation Coefficient (r)</b>
a <sub>p</sub> 443 vs. b <sub>b</sub> 442	0.820
a <sub>p</sub> 555 vs. b <sub>b</sub> 589	0.798
a <sub>p</sub> 670 vs. b <sub>b</sub> 671	0.927
b <sub>b</sub> 442 vs. Secchi depth	-0.677
b <sub>b</sub> 470 vs. Secchi depth	-0.673
b <sub>b</sub> 510 vs. Secchi depth	-0.676
b <sub>b</sub> 589 vs. Secchi depth	-0.663
b <sub>b</sub> 620 vs. Secchi depth	-0.693
b <sub>b</sub> 671 vs. Secchi depth	-0.703

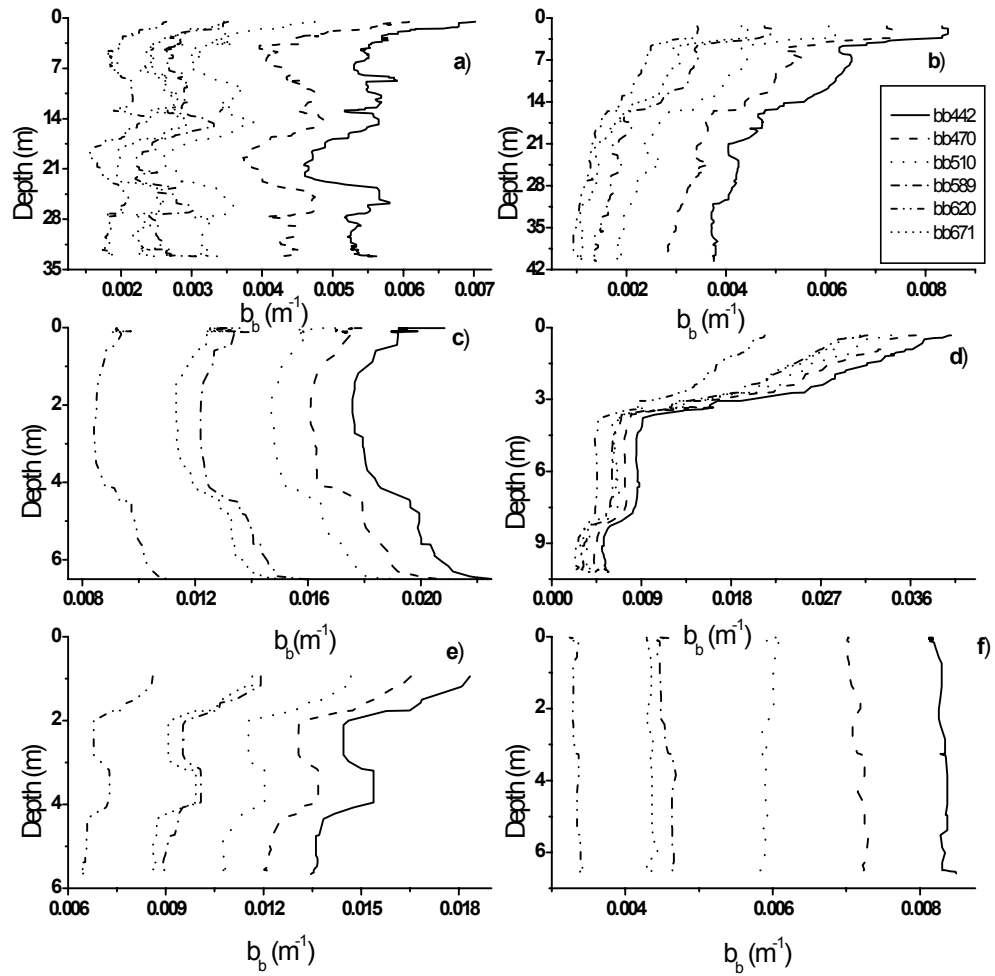


Figure 14. Profiles of the backscattering coefficient for Oceánica(a), Manchas (b), Atuneras (c), Añasco (d), Acueductos (e)and Rodríguez (f) in Mayagüez Bay during July 98. The legend at the top right corner applies to all graphs.

for Añasco station, followed by Atuneras and Acueductos stations, and the lowest values for Oceánica, Manchas and Rodriguez stations.

The profiles of the backscattering coefficient for stations 1 to 6, sampled in the October 1999 cruise, are presented in Figure 15. A trend in increasing  $b_b$  values with decreasing distance from the river mouth is clearly shown. Maximum values were found in station 4 ( $1.51 \text{ m}^{-1}$  at 442 nm). A similar pattern was found in stations 7 to 11. In this case, the station with higher  $b_b$  values was station 10, the closest to the coast, with a maximum value of  $1.26 \text{ m}^{-1}$  at 442 nm. Vertical profiles varied from nearly straight lines in the stations farther from coast to highly stratified curves at stations near to the shore. Contrasting examples of these profiles are shown in Figures 15 and 16.

Due to technical difficulties the optical package was deployed on stations 7 to 10 only. Figure 17 presents the first meter average of the total absorption coefficient (a) and beam attenuation coefficient (c) profiles. The total absorption coefficient increased as the stations approached the Yagüez River mouth. A maximum value of  $2.55 \text{ m}^{-1}$  at 412 nm was recorded in station 10. Beam attenuation coefficient, also increased toward the river mouth. The maximum value was  $12.99 \text{ m}^{-1}$  at 412 nm in station 10.

### *Apparent Optical Properties*

Remote sensing reflectance,  $R_{rs}$ , from June 1997 to January 1998, showed large spatial and temporal differences in most bands (Figure 18). Correlation analyses showed a moderate relationship between  $R_{rs}$  490 and Chl-a ( $r=0.54$ ). No other high correlations were found at other wavelengths. Although the shape of the spectral curve varied among stations and months, some trends were identified. The Oceánica station tended to maintain the shape of the  $R_{rs}$  thru the

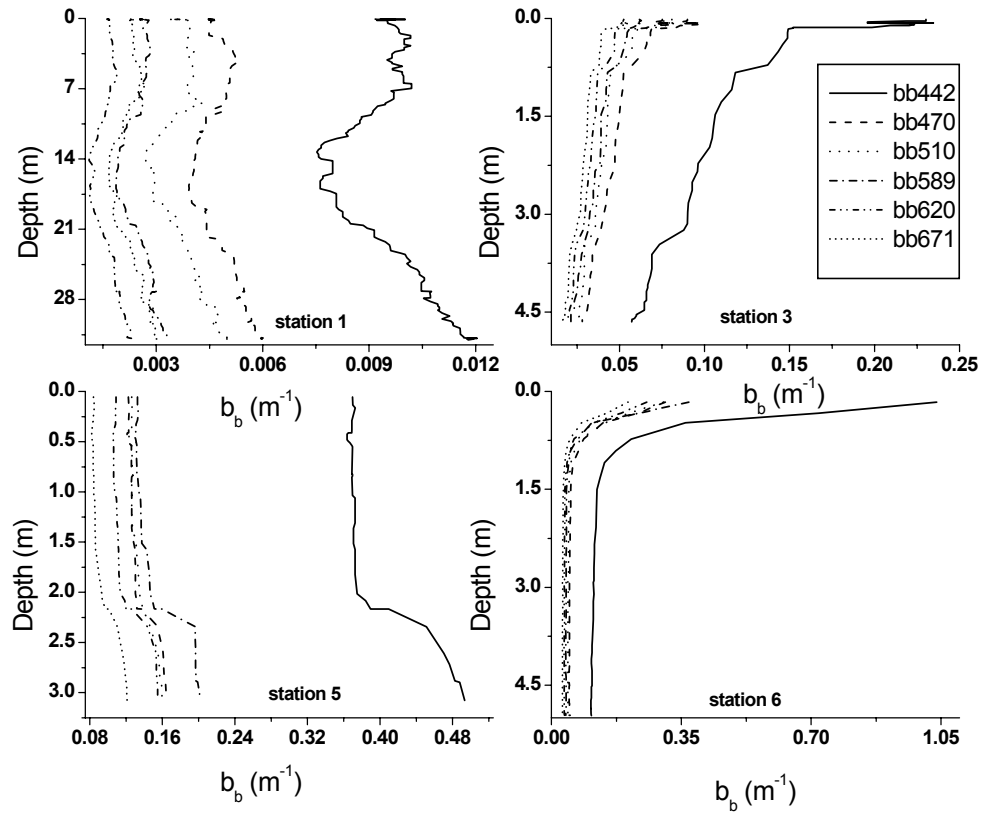


Figure 15. Profiles of the backscattering coefficient for selected stations in the Guanajibo River cruise, October 1998. The legend at the top right corner applies to all graphs.

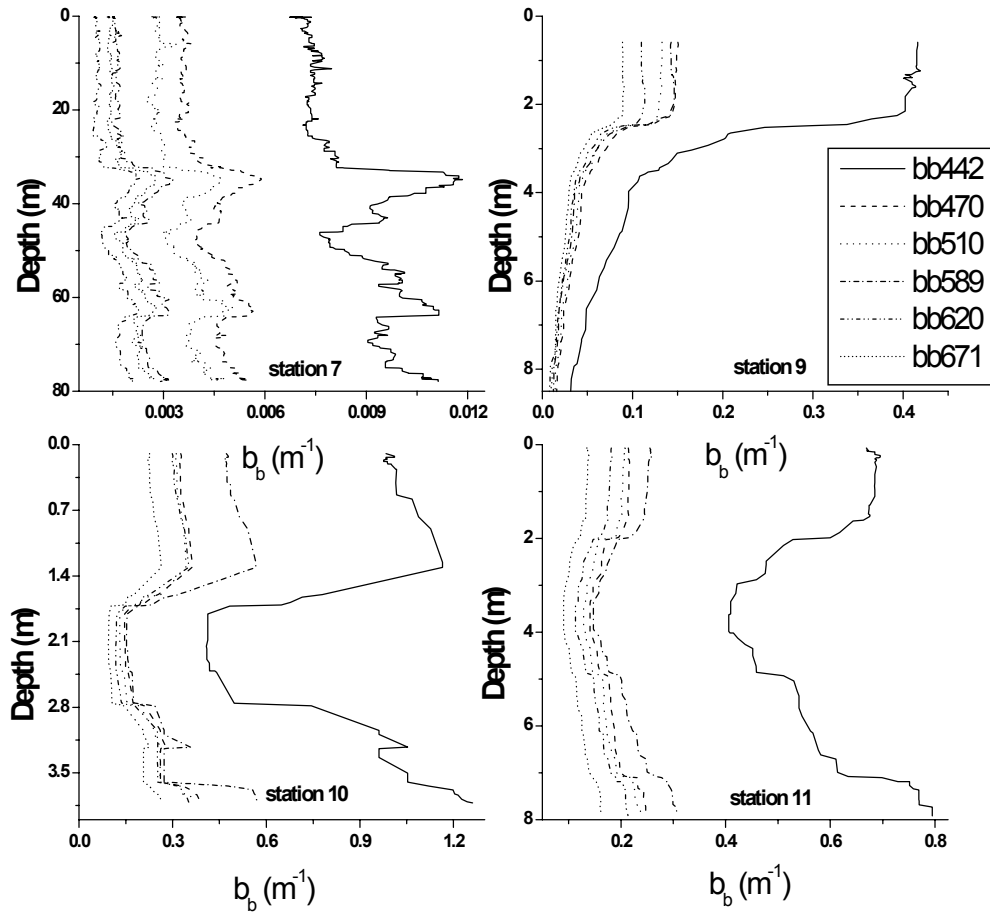


Figure 16. Selected backscattering profiles from the Yagüez River transect during October 1998. The legend at the top right corner applies to all graphs.

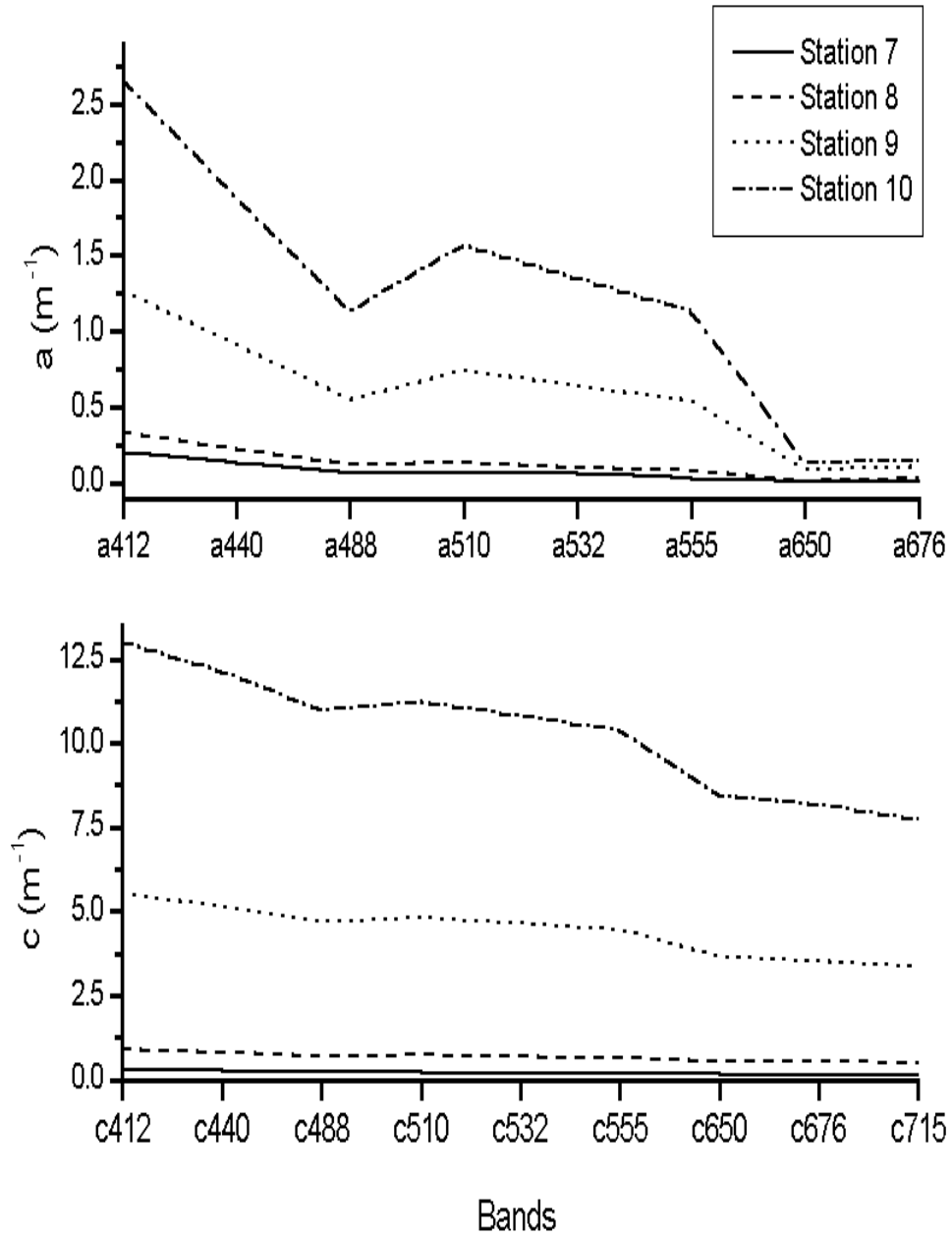


Figure 17. First meter average of total absorption coefficient ( $\text{m}^{-1}$ ) and beam attenuation coefficient ( $\text{m}^{-1}$ ), in Yagüez River stations, October 1999.

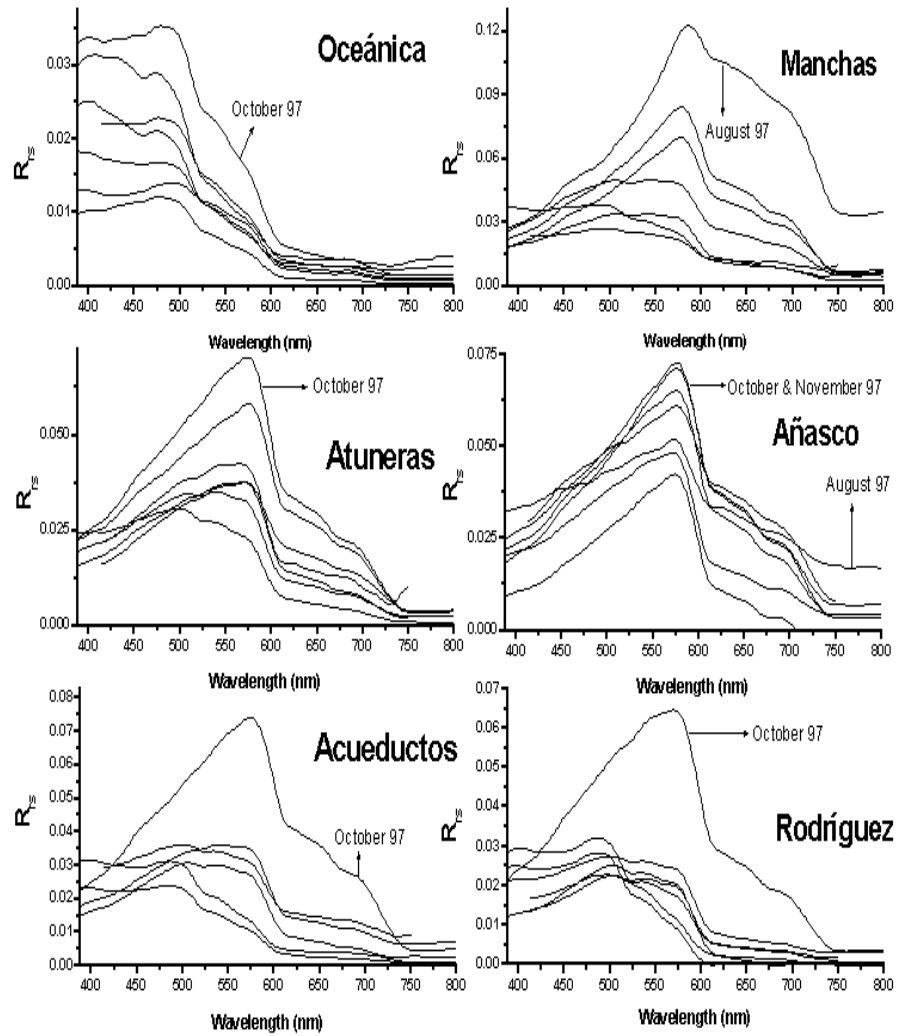


Figure 18. Remote sensing reflectance curves from June 1997 to January 1998.

year, with a broad peak around 490 nm, and very little Rrs on wavelengths above 600 nm. The other stations usually had a peak of Rrs around 550 nm, with shoulders around 700 nm. A third type of spectral shape was found in inshore stations consisting of a very broad flattened peak extending from 400 nm to 590 nm, lower in magnitude than the previous type of curve. Examples of the typical reflectance curves in Mayagüez Bay are shown in Figure 19.

The Rrs values for July 1998 are presented in Figure 20. The Añasco station showed the highest values with a definite peak around 555 nm. The lowest values were found in the Manchas station. Acueductos and Atuneras stations showed lower values in the blue region of the spectrum (412 to 490 nm), but much higher reflectance values at 555 nm than Oceánica, Manchas and Rodríguez stations.

In the October 1999 cruise, the Rrs values increased toward the shore. In the Guanajibo River stations, the highest reflectance values were found at station 4 ( $0.03 \text{ sr}^{-1}$  at 590 nm). Rrs curves show at least two types of shapes during this cruise. The first type had maximum Rrs values near 490 nm and it was associated with waters far from the river mouth. The second type had a pronounced peak around 590 nm and it was associated with waters near to the river mouth. Stations 7 to 11 showed the same pattern, station 10 with the highest reflectance values ( $0.031 \text{ sr}^{-1}$  at 590 nm). These results are presented in Figure 21.

Vertical attenuation coefficients for PAR ( $k_d$ ) were measured in this cruise. The highest  $k_d$  values were found in Añasco station ( $0.39 \text{ m}^{-1}$ ) followed by Atuneras ( $0.31 \text{ m}^{-1}$ ). In Acueductos station, a value of  $0.29 \text{ m}^{-1}$  was measured. The lowest value measured in July was  $0.11 \text{ m}^{-1}$  in the Oceánica station. This information is summarized in Table 5.

Vertical attenuation coefficient at 490 nm,  $K_d(490)$ , was calculated using the following relationship (Kirk, 1984):

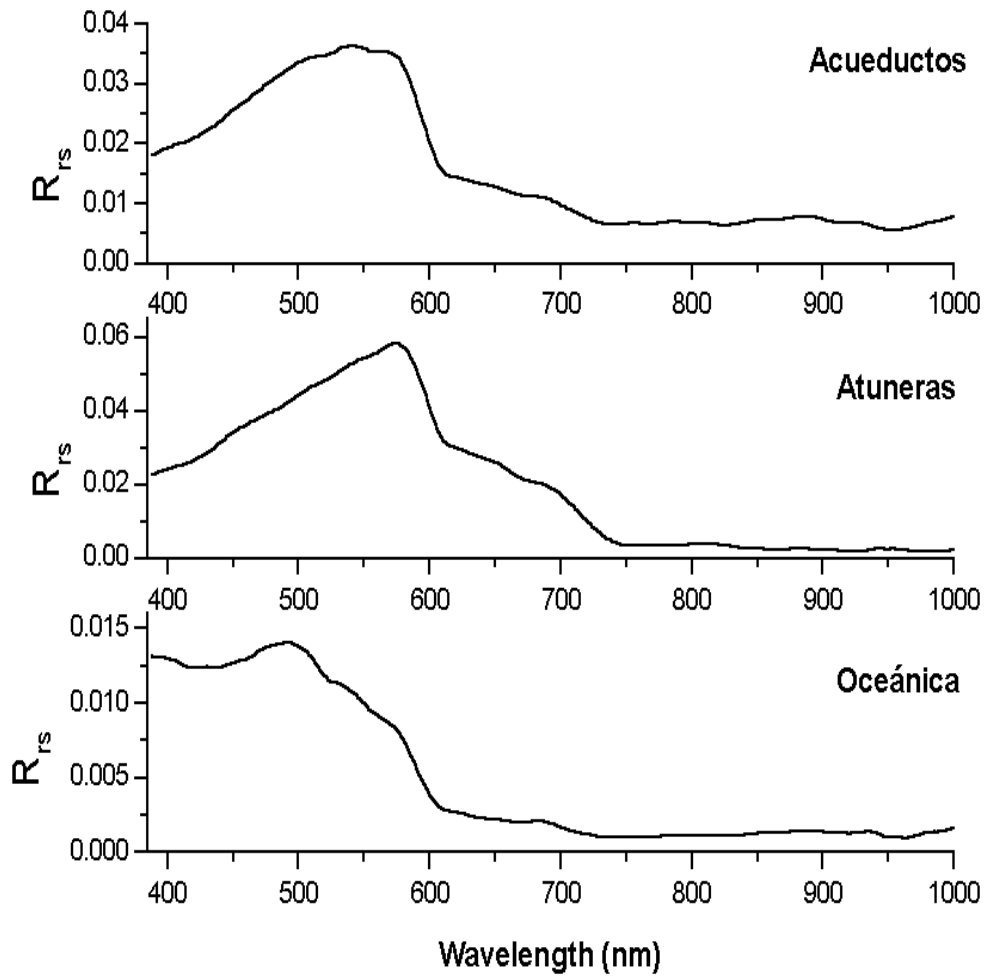


Figure 19. The three typical spectral shapes of remote sensing reflectance (R<sub>rs</sub>) curves obtained in Mayagüez Bay. These examples are from November 1997. Notice the difference in magnitudes of the y axis.

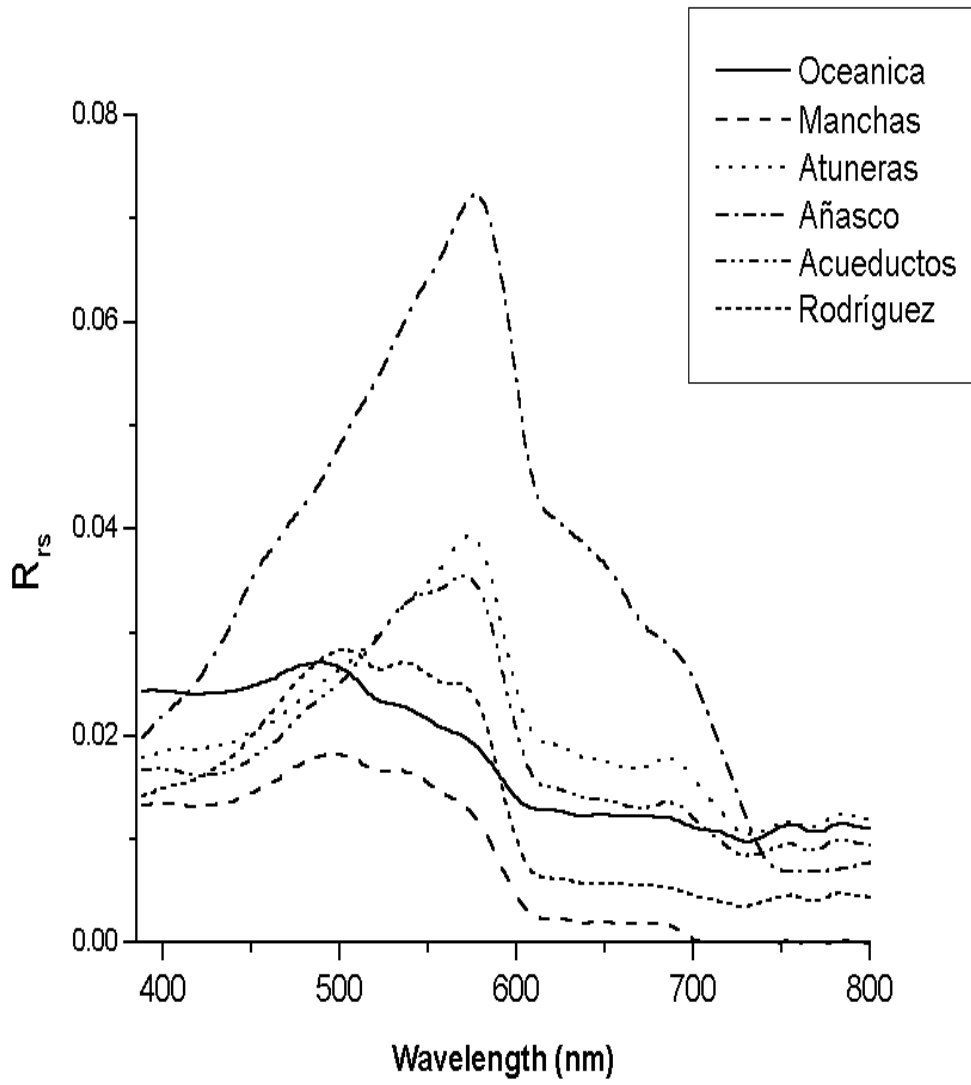


Figure 20. Remote sensing reflectance curves in Mayagüez Bay during July 1998.

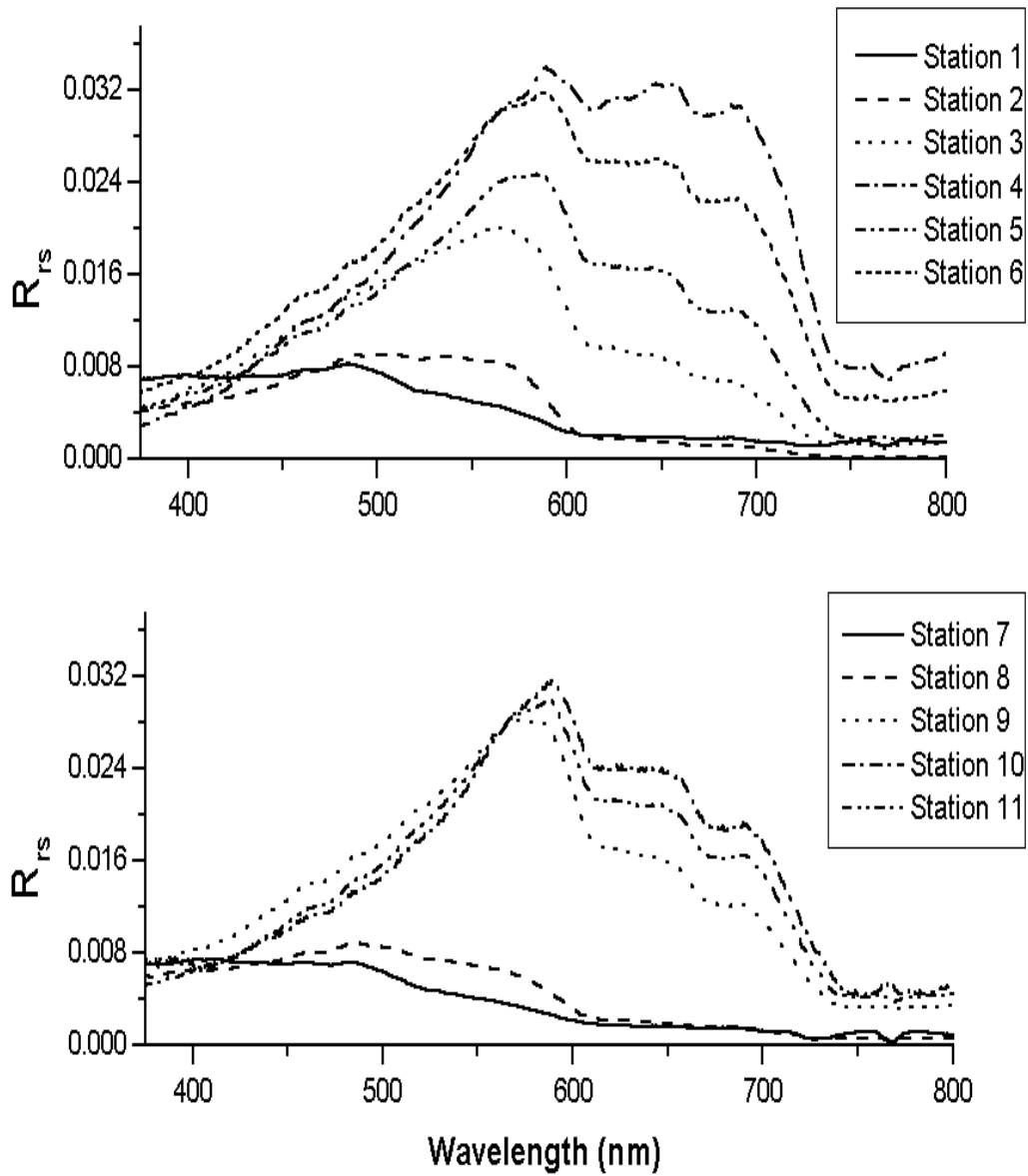


Figure 21. Remote sensing reflectance curves for the Guanajibo River stations (stations 1-6), and the Yagüez River stations (stations 7-11) during October 1999.

Table 5. Vertical attenuation coefficient and estimated euphotic zone in Mayagüez Bay during July 1998.

<b>Station</b>	<b><math>K_d</math></b>	<b><math>Z_{eu}</math> (m)</b>
Oceánica	0.11	41.8
Manchas	0.21	21.9
Atunera	0.31	14.6
Añasco	0.39	11.8
AAA	0.29	15.8
Rodríguez	0.23	20.0

$$K_d = (1/z_2 - z_1) \ln E_d(z_1)/E_d(z_2)$$

The  $K_d$  (490) ranged from 0.04 in station 8 to 1.48 in station 10. The results of these calculations are presented in Table 6.

#### *Ancillary Data*

Chl-a showed high significant differences in both space and time ( $P < 0.01$ ). The highest value was measured in Atuneras during April 1997 (= 6.39  $\mu\text{g} / \text{l}$ ). The lowest value (= 0.097  $\mu\text{g} / \text{l}$ ) was recorded at the Oceánica station during April 1997. The peaks in Chl-a were found in April and October. During July 1998, Chl-a was highest in Añasco station (5.88  $\mu\text{g}/\text{l}$ ), followed by Atuneras station (4.79  $\mu\text{g}/\text{l}$ ). The lowest values were found in Manchas station (0.63  $\mu\text{g}/\text{l}$ ). Rodriguez and Acueductos had relatively low Chl-a concentration during July 1998 (0.75 and 0.77  $\mu\text{g}/\text{l}$ , respectively).

Chl-a concentration also demonstrated the tendency of increasing as stations approached to the river mouth. Maximum values of Chl-a were recorded in station 5 (6.77  $\mu\text{g}/\text{l}$ ) and station 10 (11.75  $\mu\text{g}/\text{l}$ ). These values are summarized in Figure 22.

Salinity profiles in the bay ranged from 34.46 to 36.24 from February 1997 to January 1998. Most of the variability occurs in the first few meters. In general terms, June 1997 and January 1998 were the months with the highest salinity values while August 1997, September 1997 and November 1997 were the months with the lowest salinities at Mayagüez Bay.

In the October 1999 cruises, the mean salinity for the first meter ranged from 27.59 in Guanajibo (station 6) to 34.88 in Yagüez (station 7). Low salinity

Table 6. Vertical attenuation coefficients at 490 nm calculated for the Yagüez River transect during October 1999.

<b>Station</b>	<b><math>K_d</math> 490 nm</b>
station 7	0.201
station 8	0.044
station 9	0.853
station 10	1.479

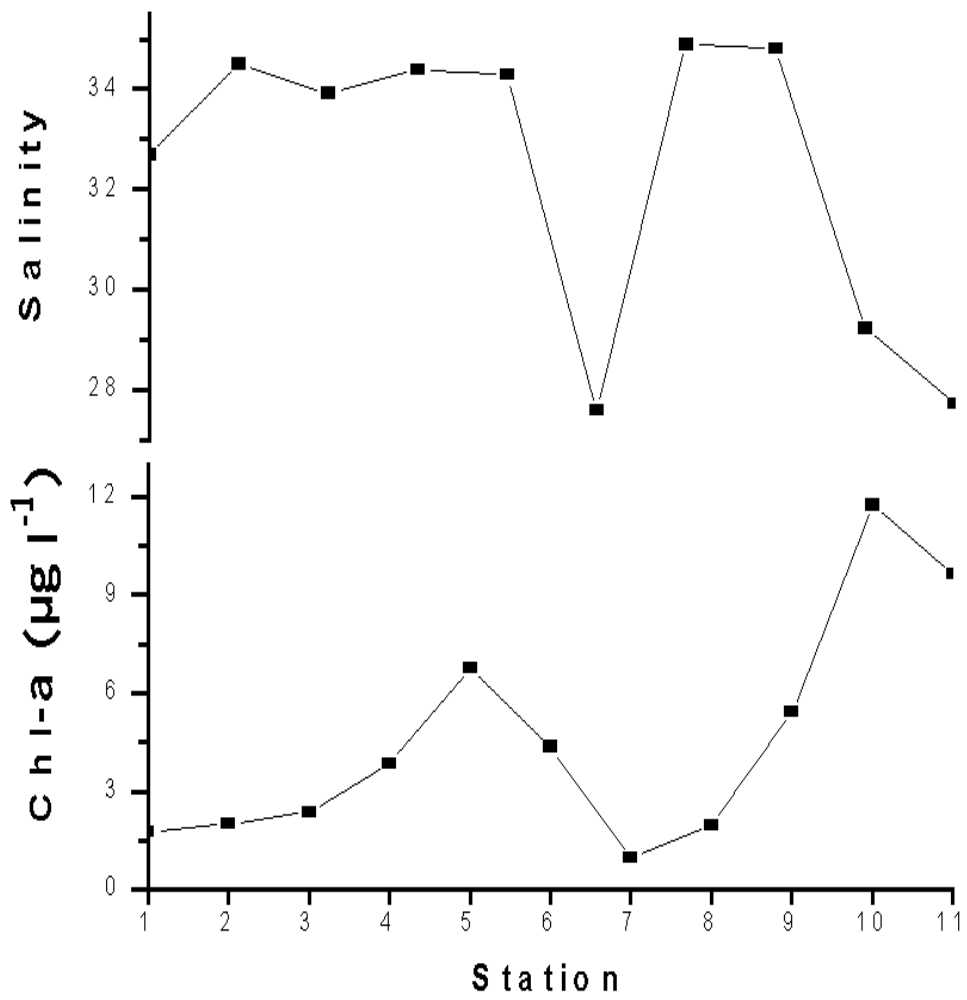


Figure 22. Chl-a concentrations and salinities at surface in Mayagüez Bay during the October 1999 cruise.

values were found in the stations closer to the Yagüez River but only at station 6 in the Guanajibo River. These results are presented in Figure 22.

From February 1997 to January 1998, Añasco River had a major discharge peak in October 1997 ( $13.55 \text{ m}^3/\text{s}$ ) and a smaller peak in August 1997 ( $9.85 \text{ m}^3/\text{s}$ ). The smallest discharge at Añasco River was measured in April ( $2.21 \text{ m}^3/\text{s}$ ). During that same period, Guanajibo River had its greater discharge in October 1997 ( $13.85 \text{ m}^3/\text{s}$ ), with a second peak occurring in August 1997 ( $3.90 \text{ m}^3/\text{s}$ ). The lowest discharge recorded in Guanajibo River during this study was  $0.71 \text{ m}^3/\text{s}$  in May 1997. In July 1998, Añasco River had a mean discharge of  $3.07 \text{ m}^3/\text{s}$  and Guanajibo River had a mean discharge of  $1.36 \text{ m}^3/\text{s}$ . These river discharge values are the average of the daily discharge for three days before the sampling. Figure 23 compares river discharge with salinity and Chl-a concentration in all stations from February 1997 to January 1998.

Suspended particulate matter (SPM) also increased as the sampling stations came closer to the river mouths. Maximum values were recorded in station 4 ( $27.6 \text{ mg/l}$ ) and station 10 ( $18.5 \text{ mg/l}$ ). These results are presented in Figure 24.

Añasco River discharge and Chl-a presented a positive correlation for Manchas station ( $r = 0.69$ ,  $n = 11$ ) and Rodríguez station ( $r = 0.74$ ,  $n = 11$ ). The other stations showed very low correlation between Chl-a and Añasco River discharge ( $r < 0.10$ ). Correlations between Añasco River discharge and Secchi disk measurements were also low ( $r < -0.50$ ).

The correlation coefficients between Guanajibo River discharge and Chl-a were high for Manchas station ( $r = 0.76$ ,  $n = 11$ ) and Rodríguez station ( $r = 0.75$ ,  $n = 12$ ). The other stations showed low correlations ( $r < 0.41$ ). Correlations between Guanajibo River discharge and Secchi depth showed a negative

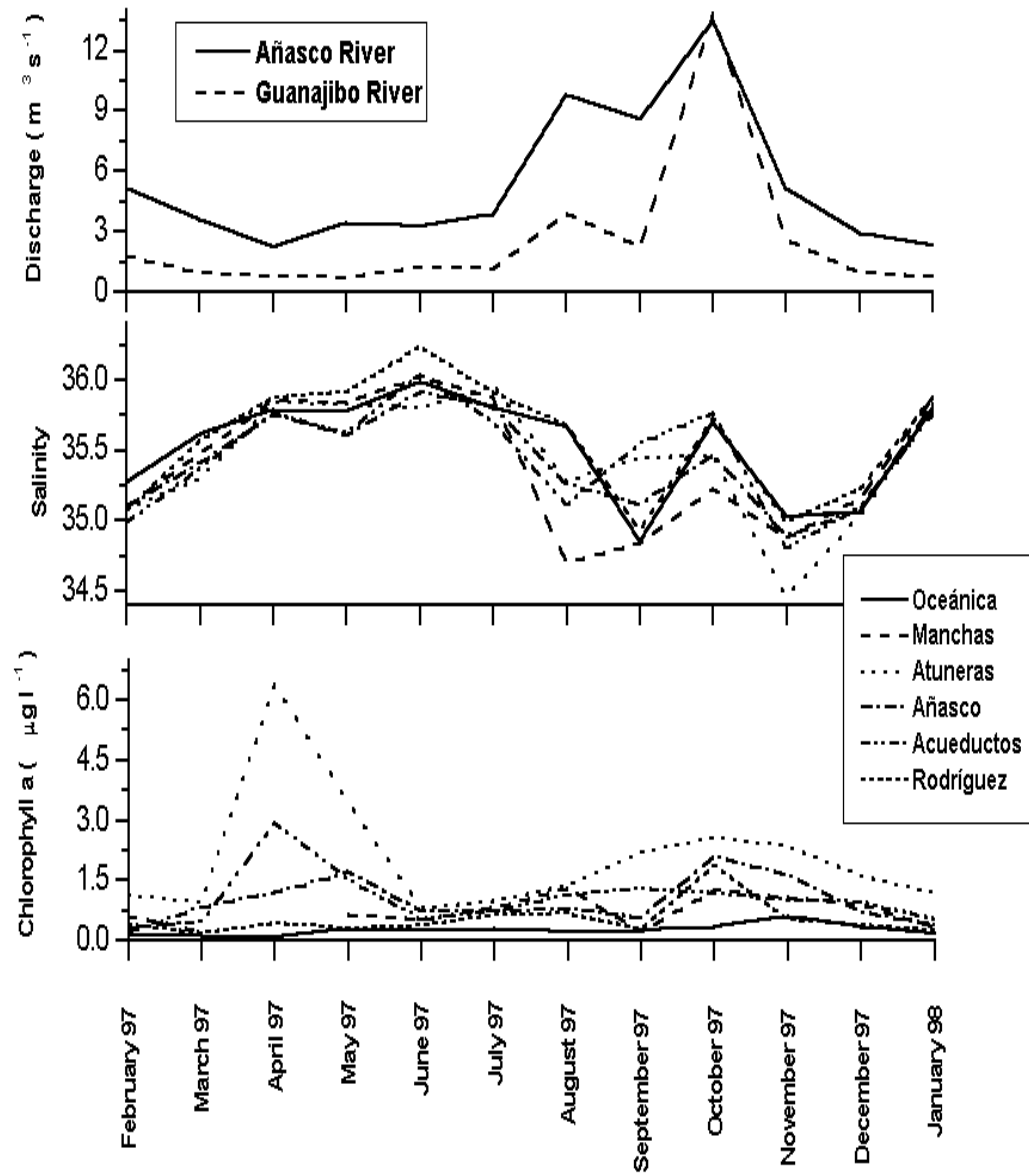


Figure 23. River discharge, salinity and Chl-a measured in Mayagüez Bay from February 1997 to January 1998.

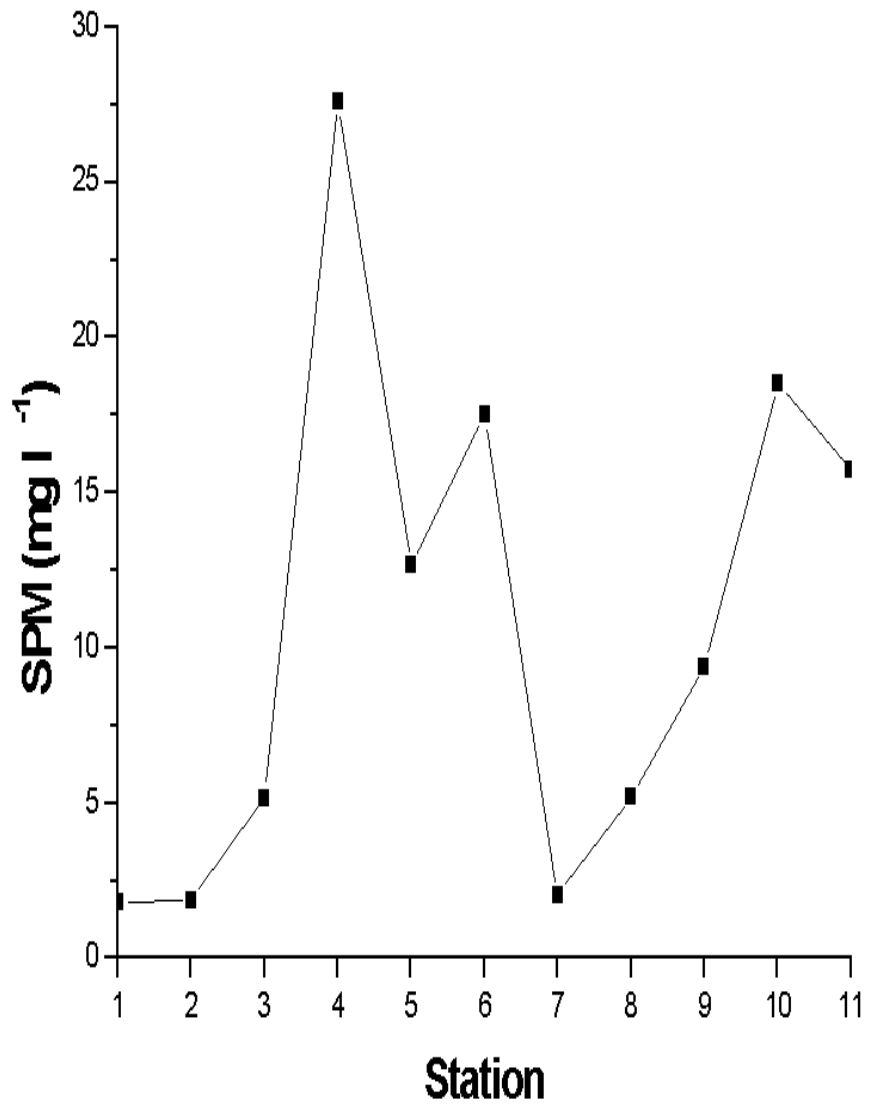


Figure 24. Suspended particulate matter (SPM) at surface in Mayagüez Bay during October 1999.

relationship with the largest coefficients in the Oceánica station ( $r = -0.60$ ,  $n = 12$ ) and Rodríguez station ( $r = -0.60$ ,  $n = 12$ ).

## DISCUSSION

Mayagüez Bay is a complex bio-optical system. The synergistic effect of rivers, industrial effluents, and coastal geomorphology creates a variety of optical provinces in a relatively small geographical area.

Absorption in the inner part of the bay is dominated by two components; detritus and CDOM. Detritus is responsible for about half of the particulate absorption in the samples from Añasco, Atuneras and Acueductos stations (Figure 25). This suggests that these three stations receive high freshwater inputs throughout the year. In Rodríguez and Oceánica stations, absorption is dominated by phytoplankton in the dry season and by detritus in the rainy season. These findings suggest that during the rainy season freshwater mixes throughout Mayagüez Bay, affecting the optical properties even in the stations farthest from the coast. Unfortunately, no CDOM measurements were taken from February 97 to January 98. In July 98, CDOM dominated absorption, being higher than particulate absorption in all stations. July 98 was an average month in terms of river discharge, with the Añasco River discharging  $3.07 \text{ m}^3 \text{ s}^{-1}$  and the Guanajibo River discharging  $1.36 \text{ m}^3 \text{ s}^{-1}$ , respectively. Since this was a dry month with average discharge, it is expected that CDOM values are considerably higher during the rainy season. These high absorptions of CDOM and detritus suggest that light is being absorbed very effectively in the blue end of the spectrum. As consequence, this filtering of blue wavelengths may stimulate phytoplankton to alter their pigment compositions in order to capture light at other wavelengths and possibly increase their Chl-a content (Kirk, 1994). This can be observed in the  $a_{ph}$  peaks around 550 and 650 nm (Figure 6). Another possible effect is the occurrence of seasonal successions of phytoplankton species in response to the varying light quality. In the October 99 cruise, it was evident that absorption

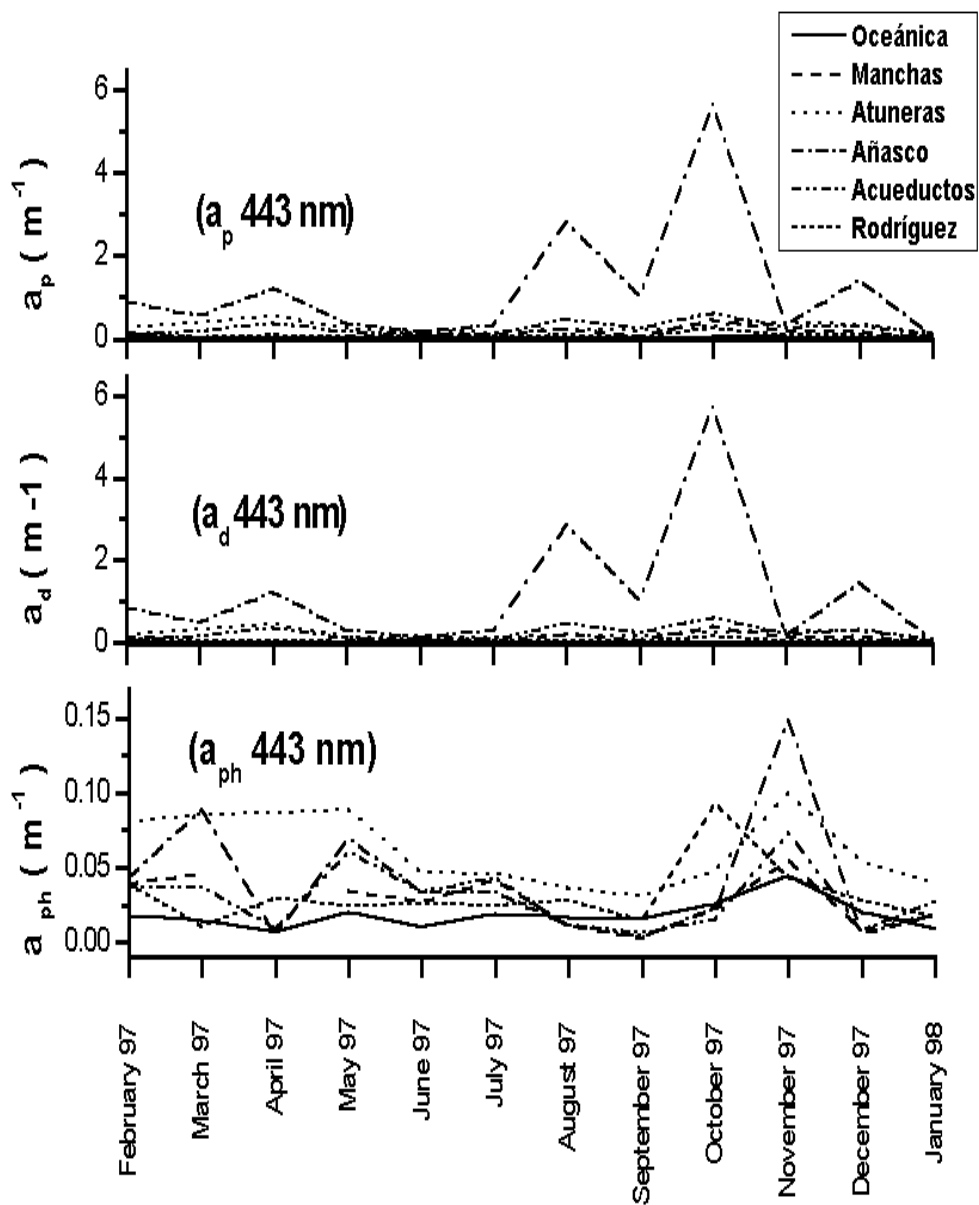


Figure 25. Comparison of particulate absorption coefficient, detritus absorption coefficient and phytoplankton absorption coefficient at 443 nm. Note the proportion of particulate absorption due to detritus.

increased toward the river mouth. This absorption was also dominated by CDOM, and detritus. October is the peak of river discharge in Mayagüez Bay. Therefore, in these highly light attenuating conditions, phytoplankton may be limited by light instead of nutrients. Notice that absorption by phytoplankton is about one order of magnitude less than particulate absorption and two orders magnitude less than CDOM absorption.

Backscattering profiles show a highly stratified distribution of particles (Figure 14). These features may be associated to sediment resuspension caused by wind or by internal waves reflected into Mayagüez Bay. This is specially feasible during the dry season, when there is not a significant input of river transported sediment into the bay, but still the particulate absorption and backscattering coefficients are high. Backscattering was very high in Atuneras, Añasco and Acueductos stations. These stations also showed the highest particulate absorption values during the course of this study. The fact that  $a_p$  and  $b_b$  are well correlated in Mayagüez Bay, suggests that a common factor regulates these parameters in the bay. Inanimate particle concentration could be this factor. This is supported if we consider the nature of the optical components in the bay. Particulate absorption in the bay is composed mostly by inanimate matter (as we discussed earlier) and phytoplankton absorption is usually low. Inanimate matter at typical concentrations does not absorb light strongly but scatters quite intensely (Kirk, 1994). At the high concentrations encountered in Mayagüez Bay, inanimate particulate matter may be very important in the absorption and scattering processes.

The remote sensing reflectance signal throws in additional evidence on the optical properties of Mayagüez Bay. Water absorbs light strongly at 750 nm, yet reflectance was far from zero at this wavelength in all stations except Oceánica (Figure 18). This was more pronounced during rainy months such as August,

November and October. This high reflectance in the red ( $\lambda > 670$  nm) is consistent with the red clay minerals washed down by local rivers. From the reflectance data we can also infer that the two stations with the higher concentration of blue absorbing components (CDOM and detritus) are Atuneras and Añasco (Figure 18). The rest of the stations only showed low reflectance in the blue during the peak of the rainy season, except Oceánica that was offshore and received the lowest impact from river run-off. It is also evident in some stations the Rrs peaks at 550 nm. These peaks are associated with high concentrations of Chl-a and are characteristic of Atuneras and Añasco stations, although in the peak of the rainy season all inshore stations showed a similar low blue, high green reflectance curve. Although these stations had higher values of absorption and backscattering (hence attenuation), they also had the highest values of Chl-a (Figure 23). In the October 1999 cruise, it was clearly shown that the magnitude of Rrs curve increased and the spectral shape transformed from a featureless curve from 350 to 600 nm to a low reflectance in the blue and a very high peak in 550 nm as the salinity (distance to the river mouth) decreased (Figure 21). This may be explained by an increase in CDOM and detritus, increasing absorption in the blue region, and an increase in nutrients, fertilizing the phytoplankton. These results are in agreement with the findings of Gilbes *et al.* (1996).

Chl-a concentrations measured at Mayagüez Bay are within those measured in other bays. Webb and Gómez (1998) reported Chl-a concentrations averaging 2  $\mu\text{g/L}$  in San Juan Bay. Gilbes *et al.* (1996) measured Chl-a concentrations up to 2.4  $\mu\text{g/L}$  in the Añasco River mouth. Chl-a peaks in October can be explained as the result of a peak in the river discharge during the rainy season (Figure 23). This explanation is supported by the findings of Gilbes *et al.* (1996). The Chl-a peak of April is more difficult to justify. The weak correlation between Chl-a and river discharge suggest that other factors besides river

discharge may play a role in the phytoplankton dynamics of Mayagüez Bay. These factors may include anthropogenic activities, wind driven sediment resuspension and internal waves.

In Mayagüez Bay, seasonal river discharge appears to be the principal factor regulating the bio-optical properties and hence the phytoplankton populations. Anthropogenic activities in the river basins alters the composition of the rivers input in the bay and therefore the characteristics of the water masses entering the bay (Kirk, 1994). The western basin of Puerto Rico is highly developed and deforested, which favors erosion and transference of soil particles into the river waters. These suspended particles increase scattering and absorption, effectively attenuating light, but also increase nutrient concentrations (Gilbes *et al.* 1996). Resuspension of sediments by wind and waves seems to be specially important in the dry season, from February to April (Alfonso, 1995, Gilbes *et al.*, 1996). Another possibility is the intrusion of internal waves into Mayagüez Bay, suspending sediments deposited earlier within the coastal zone (Edwin Alfonso, personal communication, Bogucki and Redekopp, 1999). At smaller spatial scales, the anthropogenic effects of the tuna industry and sewage processing plants may be important. Nutrients in the vicinity of the Atuneras and Acueductos station were high, specially organic nitrogen (Mónica Alfaro, unpublished data). Phytoplankton populations may be responding to increased nutrient supply at these stations. Increased predation of zooplankton by gelatinous plankton (medusae and ctenophores) may be another mechanism accounting for larger phytoplankton biomass in these stations. Large populations of these organisms has been reported in Acueductos and Atuneras station (Mónica Alfaro, unpublished data). This predation regulate abundance of zooplankton populations, resulting in lower grazing pressure over phytoplankton.

The high range of variability found in bio-optical properties in Mayagüez Bay point out the necessity of developing algorithms capable of discerning Chl-a signature from other components of the coastal aquatic environment. The complex processes occurring in the bay need to be studied in more detail in order to formulate functional relationships between Rrs and Chl-a.

## CONCLUSION

Mayagüez Bay is a highly dynamic environment from a bio-optical perspective. Spatial and temporal variability is very high in the bay. Bio-optics appear to be largely determined by river input, but anthropogenic factors may play a role at a smaller spatial scale. There is probably a synergistic effect in those stations closer to the anthropogenic influence. Other oceanographic processes may be important defining the bio-optical characteristics of the bay but river input is probably the single most important factor. Specific conclusions drawn from this work are:

1. Bio-optical properties are highly variable in Mayagüez Bay and are related to river discharge.
2. There are high correlations between absorption and backscattering in the bay, but no clear pattern of correlations were found. This is probably the result of the bio-optical complexity of the bay.
3. Although some data may suggest the possibility of light limitation of phytoplankton communities in the bay, there is no clear evidence in this study. This subject needs more research.

Future studies should take into account vertical variability in optical properties and what effects, if any, it has on the values observed at surface. It is also recommended to study taxonomical composition of phytoplankton assemblages in the bay and perform photosynthetic efficiency and primary production studies. Other studies that may provide essential data and should be considered in the future are photosynthetic pigment analysis using the HPLC method and nutrients analysis.

## REFERENCES

- Ackleson S. G., 1998. Variability in the inherent optical properties of ocean waters around Lee Stocking Island, Bahamas. *Ocean Optics XIV*, Kailua-Kona, Hawaii.
- Alfonso E., 1995. The coastal current regime in Añasco Bay during a one year period. Master of Science Thesis. UPRM. Department of Marine Sciences.
- Banse, K., and English D. C. 1994. Seasonality of coastal zone color scanner phytoplankton pigment in the offshore oceans. *J. of Geophysical Research*, 99(C4): 7323-7345.
- Bogucki, D. J., and Redekopp L. A 1999. A mechanism for sediment resuspension by internal solitary waves. *Geophysical Research Letters* 26(9): 1317-1320.
- Bricaud, A., Morel A. and Prieur L. 1981. Absorption by dissolved organic matter of the sea (yellow substance) in UV and visible domains. *Limnol. Oceanogr.* 26: 43-53.
- Bricaud, A. and Stramski, D. 1990. Spectral absorption coefficients of living phytoplankton and nonalgal biogenous matter: A comparison between the Peru upwelling and the Sargasso Sea. *Limnol. Oceanogr.*, 35(3): 562-582.
- Carder, K. L., Steward, R. G., Harvey, G. R., & Ortner, P. B. (1989). Marine humic and fulvic acids: Their effects on remote sensing of ocean chlorophyll. *Limnol. Oceanogr.*, 34: 68-81.
- Del Castillo C. E., Coble P. G., Morell J. M., López J. M. and J. E. Corredor. 1999. Análisis of the optical properties of the Orinoco River Plume by absorption and fluorescence spectroscopy. *Marine Chemistry*, 66: 35-51.
- Denny M. W. 1993. *Air and Water, The biology and physics of life's media*, Princeton University Press, Princeton, New Jersey 341 pp.
- D'Sa E. J., Steward R. G., Vodacek A., Blough, N. V. and Phiney D. 1999. Determining optical absorption of colored dissolved organic matter in seawater with a liquid capillary waveguide. *Limnol. Oceanogr.*, 44(4): 1142-1148.

- Eppley, R. W. 1977. The growth and culture of diatoms, in the biology of diatoms, Werner, D., Ed., Blackwell Scientific, Oxford.
- Figueiras, F. G., and Arbones B. 1999. Implications of bio-optical modeling of phytoplankton photosynthesis in Antarctic waters: Further evidence of no light limitation in the Bransfield Strait. *Limnol. Oceanogr.*, 44(7): 1599-1608.
- García, C. A., V. M. García, A. S. González and Omachi C. Y. 1998. Bio-optical characteristics of southern Brazilian waters. *Ocean Optics XIV*, Kailua-Kona, Hawaii.
- Garrison, D. L. 1984. Planktonic Diatoms, in *Marine Plankton Life Cycle Strategies*, Steidinger, K. A. and Walker L. M., Eds., CRC Press, Boca Raton, Florida.
- Gilbes, F., López, J. M. and Yoshioka P. 1996. Spatial and temporal variations of phytoplankton chlorophyll a and suspended particulate matter in Mayagüez Bay, Puerto Rico. *J. of Plankton Res.* 18: 29-43.
- Gordon, H. R., Clark D. K., Brown J. W., Brown O. B., Evans R. H., and Broenkow W. W. 1983. Phytoplankton pigment concentrations in the Middle Atlantic Bight: comparisons of ship determinations and CZCS estimates. *Applied Optics*, 22(1): 20-36.
- Gordon, H. R. and Morel, A. Y. 1983. Remote assessment of ocean colour for interpretation of satellite imagery. A review. Springer, New York.
- Grove, K., 1977. Sedimentation in Añasco Bay and river estuary: Western Puerto Rico. Master of Science Thesis. UPRM. Department of Marine Sciences.
- Kirk, J. T. O. 1994. *Light and Photosynthesis in Aquatic Ecosystems*. Cambridge University Press, Cambridge.
- Levinton, J. S. 1982. *Marine Ecology*. Prentice-Hall, New York.
- Li, Y. and T. J. Smayda. 1998. Temporal variability of chlorophyll in Narrangansett Bay, 1973-1990. *ICES Journal of Marine Science*, 55: 562-573

- Longhurst, A.R., and Pauly D. 1987. Ecology of the tropical oceans. Academic Press Inc. San Diego. 407 pp.
- Kishino, M., Okami N. and Ichimura S. 1985 Estimation of the spectral absorption coefficients of phytoplankton in the sea. *Bull. Mar Sci.* 37: 634-642.
- Mitchell, B. G. and Kiefer, D. A. 1984. Determination of absorption and fluorescence excitation spectra of phytoplankton. In: *Marine phytoplankton and productivity*. Holm-Hansen, O., Bolis L., Giles R. (Ed.) Springer-Verlag, Berlin. 157-169 pp.
- Morel, A. 1987. Chlorophyll-specific scattering coefficient of phytoplankton. A simplified theoretical approach. *Deep-Sea Res.* 34: 1093-1105.
- Morelock, J., Grove, K., and Hernández, M. L. 1983. Oceanography and patterns of shelf sediments in Mayagüez, Puerto Rico. *J. Sed. Petrol.* 53: 371-381
- Nybakken, J. W. 1993. *Marine Biology An ecological approach*. Harper Collins, New York. 462 pp.
- Platt, T. [ED.] 1981. Physiological bases of phytoplankton ecology. *Can. Bull. Aquat. Sci.* 210: 346p.
- R. M. Pope and Fry, E. S.. 1997. Absorption spectrum (380-700 nm) of pure water. II. Integrating cavity measurements. *Appl. Opt.*,36: 8710-8723
- Raymont, J. E. G. 1980. *Plankton and productivity in the oceans*, 2ed. Vol. 1 Pergamon Press, Oxford.
- Smayda, T.J. 1970. The suspension and sinking of phytoplankton in the sea, *Oceanogr. Mar. Biol. Ann. Rev.*, 8(853).
- Steidinger, K.A. and Walker, L.M. 1984. Introduction, in *Marine plankton life cycle strategies*, Steidinger, K.A. and Walker, L.M., Eds., CRC Press, Boca Raton, Florida
- Sumich, J.L. 1984. *Biology of Marine Life* Wm. C. Brown Publishers, Dubuque, Iowa 386 PP.

Thurman, H.V. and Webber, H.H. 1984. Marine Biology, Charles E. Merrill, Columbus, Ohio

Walker, L. M. 1984. Life histories, dispersal and survival in marine, planktonic dinoflagellates, in Marine plankton life cycle strategies, Steidinger, K.A. and Walker, L.M., Eds., CRC Press, Boca Raton, Florida

Webb, R. M. T. and Gómez F. 1998. Synoptic survey of water quality and bottom sediments, San Juan Bay Estuary System, Puerto Rico, December 1994-July 1995. U.S. Geological Survey, Water-Resources Investigations Report 97-4144

Weidemann, A. D. and Bannister, T. T. 1986. Absorption and scattering coefficients in Irondequoit Bay. Limnol. Oceanogr., 31(3): 567-583.

Welschmeyer, N. A. 1994. Fluorometric analysis of chlorophyll *a* in the presence of chlorophyll *b* and pheopigments. Limnol. Oceanogr. 39(8): 1985-1992.